

CHAPTER VII

THE VENUS IONOSPHERE

S. J. Bauer,¹ L. M. Brace,² H. A. Taylor, Jr,²
T. K. Breus,³ A. J. Kliore,⁴ W. C. Knudsen,⁵ A. F. Nagy,⁶
C. T. Russell⁷ and N. A. Savich⁸

¹ *Institute for Meteorology and Geophysics, University of Graz and Space Research Institute, Austrian Academy of Sciences, A-8010 Graz, Austria*

² *NASA, Goddard Space Flight Center, Greenbelt, MD 20771, U.S.A.*

³ *Space Research Institute, U.S.S.R. Academy of Sciences, Moscow 117810, U.S.S.R.*

⁴ *Jet Propulsion Laboratory, Pasadena, CA 91109, U.S.A.*

⁵ *Knudsen Geophysical Research, Monte Sereno, CA 95030, U.S.A.*

⁶ *University of Michigan, Ann Arbor, MI, U.S.A.*

⁷ *IGPP, University of California, Los Angeles, CA 90024, U.S.A.*

⁸ *Institute of Radioengineering and Electronics, U.S.S.R. Academy of Sciences, Moscow, U.S.S.R.*

ABSTRACT

Physical properties of the Venus ionosphere obtained by experiments on the US Pioneer Venus and the Soviet Venera missions are presented in the form of models suitable for inclusion in the Venus International Reference Atmosphere. The models comprise electron density (from 120 km), electron and ion temperatures, and relative ion abundance in the altitude range from 150 km to 1000 km for solar zenith angles from 0° to 180°. In addition, information on ion transport velocities, ionopause altitudes, and magnetic field characteristics of the Venus ionosphere, are presented in tabular or graphical form. Also discussed is the solar control of the physical properties of the Venus ionosphere.

1. Introduction

Following the detection of an ionosphere of Venus by the radio occultation experiment on Mariner 5 (Mariner Stanford Group 1967; Kliore et al., 1967), the Mariner 10 fly-by mission (Howard et al. 1974; Fjeldbo et al. 1975), the Venera 9 and 10 (Aleksandrov et al. 1976a) and the Pioneer Venus radio occultation observations (Kliore et al., 1979) have provided most of the statistical information on the behavior of the electron density maximum as function of solar zenith angle and solar activity.

The radio occultation observations are the only ones that provide data below the main peak occurring at an altitude of ~140 km, whereas the in-situ observations of the Venus ionosphere of the Pioneer Venus orbiter are largely restricted to altitudes \geq 150 km (Colin, 1980).

Exhaustive reviews of our knowledge of the Venus ionosphere based on the Pioneer Venus mission are contained in the "Venus book" (Hunten et al., 1983, Ch. 23-26).

Neither radio occultation observations (on any spacecraft) nor in-situ experiments on the Pioneer Venus orbiter provide true vertical profiles. In the first case, assumptions regarding spherical symmetry have to be made in recovering electron density profiles. In the case of in-situ measurements on the Pioneer Venus orbiter, these are made along the trajectory near periaxis where horizontal displacements or representative 'altitudes' along the orbit are relatively small but not negligible. Here again horizontal gradients may be of some significance. Bearing these limitations in mind, Pioneer Venus orbiter measurements provide the only data on ion composition, electron and ion temperatures, ion transport velocities, and magnetic field characteristics of the Venus ionosphere.

In spite of some inherent problems regarding different spatial resolution and characteristics of in-situ experiments on the Pioneer Venus Orbiter (Breus et al., 1983), the VIRA Task Group on Ionosphere and Solar-Wind Interaction decided at its meeting during the IUGG at Hamburg (1983), to proceed with an empirical model of the Venus ionosphere based on all available data. In the following tables and figures, ionospheric parameters will be presented that are derived from a large statistical base (more than three years of PVO in-orbit operations) augmented with radio occultation data from both the Veneras and Pioneer Venus orbiter (Kliore, 1984; Savich, 1984).

2. The Main Layer of Ionization

2.1 Dayside Ionosphere

There is now general agreement that the dayside ionospheric peak of Venus results from photochemical processes and can therefore be described to first order by a Chapman layer

(Ivanov-Kholodny et al., 1979; Cravens, Kliore, et. al., 1981; Nagy, Cravens, and Gombosi, 1983; Brace et al., 1983).

Accordingly, the ionospheric peak density N_m and its height h_m should follow the prescribed Chapman-layer behavior as function of the solar zenith angle X , viz. $N_m \sim \cos^{1/2} X$ and $h_m \sim \ln \sec X$.

A compilation of radio occultation data from Venera 9 and 10 and Pioneer Venus (Cravens, Kliore, et. al., 1981) shows very good agreement of $N_m(X)$ with a Chapman layer behavior, but the zenith angle dependence of the height of the ionization peak, h_m , is less satisfactory. Departures from a simple Chapman-layer behavior are to be expected for the Venus ionosphere, since the principal ion (O_2^+) differs from the principal ionizable constituent (CO_2) and since the scale height, H , is variable due to zenith angle (and solar activity) dependence of the exospheric temperature. It should be also noted that during the Venus day, there occur several 27-day rotation cycles and thus a solar modulation will be apparent (Bauer and Taylor, 1981).

According to an analysis of the departures from an ideal Chapman layer behavior (Bauer, 1983), the solar zenith angle control of the Venus ionosphere obeys the relations

$$N_m \sim \cos^k X \quad (1)$$

with $k > 0.5$

and

$$h_m(X) = h_o + H_o \cos^n X \ln \sec X \quad (2)$$

where the subscripts refer to $X = 0$.

The exponents $k = 0.55$ and $n = 0.2$ (which are also consistent with theoretical considerations, Bauer, 1983) appear to provide the best fit to the observations as shown in Figures 7-1 and 7-2. The dependence of the peak density for overhead sun ($X = 0$), N_o , as function of solar activity, represented by the solar 10.7 cm flux, $F_{10.7}$, has been shown empirically to correspond to values of slope

$$m = d \ln N_o / d \ln F_{10.7} \quad (3)$$

ranging between $m = 0.5$ (ideal Chapman layer) and $m = 0.3$. Theoretical arguments by Bauer (1983) for an ionospheric layer, whose principal ion is O_2^+ favor $m = 0.36$ (if the principal ion were CO_2^+ then $m = 0.43$), in good agreement with the data (Figure 7-3). A comparison of N_O with actually measured solar EUV fluxes, yields a similar dependence, $m = 0.33$ (Elphic et al., 1983). The relationship of ionospheric peak parameters and solar zenith angle and solar activity could thus be used with some confidence for predictive purposes.

2.2 Night-Side Ionosphere

The discovery of a night-side ionosphere of Venus by the radio occultation experiment on Mariner 5 came as somewhat of a surprise in view of the long Venus night (~58 days). Of various proposed mechanisms for the maintenance of the night-side ionosphere only two plausible ones, in terms of the observed characteristics, remain: the main peak is probably formed by ionizing fluxes of electrons with energies of several tens of electron volts as measured on Venera 9 and 10 (Gringauz et al., 1977) and Pioneer Venus (Intriligator et al., 1979; Cravens, Nagy, et al., 1981; Spenner et al., 1981) as argued by Gringauz et al., (1983) and the transport of the dominant ion O^+ in the upper ionosphere from the day-side to the night-side with subsequent downward diffusion and charge exchange with CO_2 or N_2 (Spenner et al., 1981; Taylor, Jr. et al., 1982; Cravens et al., 1983; Nagy and Cravens, 1984). O^+ -fluxes from the day-side across the terminator with velocities of kilometers per second have been observed on Pioneer Venus (Knudsen et al., 1980; Knudsen et al., 1982) as shown in Figure 7-4.

The principal characteristic of the night-side ionosphere is its high variability; sometimes it seems to disappear altogether. The fact that O^+ and H^+ ions are also present on the night-side argues for their supply from the day-side. The variability of the night-side ionosphere is illustrated in Figure 7-5, which shows data obtained by the Pioneer Venus radio occultation experiment (Kliore, 1982, Kliore, et al., 1979).

3. The Structure of the Venus Top-Side Ionosphere

3.1 The Ionopause

One of the most unique features of the Venus ionosphere is its direct interaction with the solar wind. This feature has already been recognized in the early Mariner 5 data; long-term observations by Venera and Pioneer Venus experiments have delineated the variability of this interface, called the ionopause. To first order, it occurs where there is approximate equality between the solar wind pressure $p_{sw} = (\rho v^2)_{sw} \cos^2 X$ and the ionospheric plasma pressure $p_{ion} = N k (T_e + T_i)$, where N is the ionospheric plasma density, T_e and T_i the electron and ion temperatures and k , Boltzmann's constant. Detailed balance is provided by considering the 'magnetic pressure' $p_B = B^2/8\pi$ of the piled-up interplanetary magnetic field. (Russell and Vaisberg, 1983). The height of the day-side ionopause h_{ip} can be expressed in terms of magnetic pressure p_B (Elphic et al., 1980) by

$$h_{ip} = A + B \exp (-C p_B), \quad (4)$$

(where A , B and C are constants), i.e., an increasing h_{ip} with lower p_B . Empirically derived behavior of ionopause altitude as a function of solar zenith angle shows a 'flattening' beyond the terminator. The empirical curve in Figure 7-6 is based on a statistical sample of seven Venus years observations of ionopause altitudes (Brace, 1984; Theis et al., 1984). However, there are occasions when the ionopause is at 250 km for all dayside solar zenith angles, implying an absolute lower limit.

3.2 Magnetic Field Structure Within The Ionosphere

When the ionopause is low, i.e. for low zenith angles and during periods of high solar wind dynamic pressure, the low altitude ionosphere is magnetized by currents driven in the ionosphere. This is illustrated in Figure 7-7 where the magnetic field strength B in the lower ionosphere reaches more than 100 nT while the solar zenith angle dependence of is shown in Figure 7-8 (Russell and Vaisberg, 1983). (The distribution of these currents within the ionosphere may be described by the model of Luhman et al. (1984), and Cravens et al. (1984). Such a magnetic field imbedded in the ionosphere also leads to

compressions of the ionosphere by a ($j \times B$) force which exhibits itself by reduced scale heights (Hartle *et al.*, 1980).

3.3 Ion Composition

The ion mass spectrometer on Pioneer Venus has identified about a dozen ions in the Venus ionosphere (Taylor, Jr. *et al.*, 1979). A typical example is presented in Figure 7-9.

Theoretical interpretation of the observed density profiles has met with reasonable success (Bauer *et al.*, 1979; Nagy *et al.*, 1983). There is appreciable variability in the ion concentration profiles. However, the main features are, the predominance of O_2^+ in the main layer, and O^+ in the topside ionosphere and increasing importance of H^+ in the night-side, particularly in the dawn region (Taylor, Jr. *et al.*, 1982).

It has recently been argued that the absolute concentration of heavy ions measured by the ion mass spectrometer in the region above the peak may be too high, possibly due to instrumental and/or environmental effects (Miller *et al.*, 1984). It is presently not known to what extent the lighter ions may also be affected; the relative abundance of lighter ions below 200 km may therefore possibly be higher than indicated by the ion mass spectrometer measurements.

3.4 Electron and Ion Temperatures

The temperatures of charged particles are measured on the Pioneer Venus orbiter by the Langmuir Electron Temperature Probe (Brace *et al.*, 1980) and the Retarding Potential Analyzer (T_i) (Knudsen *et al.*, 1979).

Theoretical interpretation of electron and ion temperatures in terms of the energetics of the Venus upper atmosphere has been very successful (Knudsen *et al.*, 1979; Nagy *et al.*, 1979; Cravens *et al.*, 1980). This is illustrated in Figure 7-10. Near the antisolar point the ion temperatures are greater than the electron temperatures. This seems to be the result of thermalization of high velocity ions coming from the day-side (Knudsen *et al.*, 1980).

A detailed empirical model for electron temperatures based on

PVO observations, has been given by Theis et al. (1984), and for ion temperatures by Miller et al. (1984).

4. The VIRA Model Ionosphere

In the following, we present an empirical model of the structure of the Venus ionosphere based on observational data from Pioneer Venus and Venera 9 and 10 experiments. Although there is great variability in the data, the large statistical sample of data (6 to 7 Venus days/years), with generally two measurements profiles every 24 hours) for the in-situ measurements at altitudes from above 150 km, together with electron density profiles from radio occultations from below 150 km, allows for mean characteristics for given zenith angle ranges to be derived.

The model for electron (plasma) density (N_e) was compiled from Pioneer Venus orbiter in-situ Langmuir probe measurements above 150 km (Brace, 1984; Theis et al., 1984) normalized at 750 km to the electron density data from PVO radio occultation data (Kliore, 1984) with 'smoothing' performed in the range of transition. Table 7-1 presents electron density (N_e) and its standard deviation from 120 km to 200 km for solar zenith angle (SZA) ranges from SZA = 0° to 120° .

Table 7-2 presents electron density, N_e , electron temperature, T_e , ion temperature, T_i , and their standard deviations for the altitude range from 150 km to 1000 km for the solar zenith angle range from SZA = 0 to SZA = 180, grouped in 20° steps of SZA. The electron temperatures (T_e) are based on Langmuir probe data (Brace, 1984; Theis et al., 1984), while the ion temperatures (T_i) are based on the Retarding Potential analyzer experiment on PVO (Knudsen, 1984). (Some of these data are extrapolated to altitudes and zenith angles where observations were lacking.)

In addition, Table 7-2 provides relative ion abundance from the PVO Ion Mass Spectrometer Experiment (Taylor, 1984) for the principal "heavy" and "light" ions in the Venus ionosphere (O_2^+ , O^+ and H^+) for the same altitude and zenith angle ranges. (Ions not tabulated [see Figure 7-9] make up another 10% of the total.) Figures 7-11 and 7-12 show graphical representations of the tabulated electron density data for two zenith angle ranges and Figure 7-13 a composite of N_e for all zenith angle ranges in Table 7-2. Figures 7-14 to 7-16 show graphical

representations of electron and ion temperatures (T_e , T_i) and Figures 7-17 to 7-20 graphical representations of relative ion abundance for selected solar zenith angle (SZA) ranges listed in Table 7-2.

In spite of some inherent shortcomings, our model embodies the best and most comprehensive data set of physical parameters of the Venus ionosphere available and thus representative mean conditions for a period of approximately five Earth years (1978-1983) of observations.

Table 7-1. Day-side Electron Densities In the Peak Region

Altitude (km)	SZA = 0° - 30°		Altitude (km)	SZA = 30° - 50°	
	Average El. Dens. (cm ⁻³)	El. Dens. Std. Dev. (cm ⁻³)		Average El. Dens. (cm ⁻³)	El. Dens. Std. Dev. (cm ⁻³)
120	2.1(5)	2.8(4)	120	1.8(5)	3.5(4)
125	2.8(5)	1.9(4)	125	2.6(5)	3.2(4)
130	3.9(5)	1.8(4)	130	3.5(5)	2.9(4)
135	5.2(5)	3.2(4)	135	5.0(5)	4.4(4)
140	6.5(5)	3.5(4)	140	5.8(5)	3.4(4)
145	6.0(5)	2.7(4)	145	5.2(5)	2.8(4)
150	4.5(5)	2.0(4)	150	3.8(5)	2.3(4)
155	3.4(5)	1.6(4)	155	3.0(5)	1.7(4)
160	2.6(5)	1.2(4)	160	2.5(5)	1.5(4)
165	2.1(5)	5.0(3)	165	2.1(5)	1.6(4)
170	1.8(5)	1.1(4)	170	1.8(5)	1.8(4)
175	1.6(5)	5.6(3)	175	1.6(5)	1.9(4)
180	1.5(5)	7.3(3)	180	1.5(5)	2.0(4)
185	1.3(5)	1.0(4)	185	1.3(5)	2.2(4)
190	1.2(5)	1.7(4)	190	1.2(5)	2.2(4)
195	1.1(5)	2.1(4)	195	1.1(5)	2.0(4)
200	9.9(4)	2.5(4)	200	9.8(4)	1.8(4)

Altitude (km)	SZA = 50° - 70°		Altitude (km)	SZA = 70° - 80°	
	Average El. Dens. (cm ⁻³)	El. Dens. Std. Dev. (cm ⁻³)		Average El. Dens. (cm ⁻³)	El. Dens. Std. Dev. (cm ⁻³)
120	1.1(5)	2.2(4)	120	6.7(4)	3.0(4)
125	1.9(5)	2.3(4)	125	1.3(5)	3.0(4)
130	2.8(5)	3.1(4)	130	2.2(5)	3.8(4)
135	3.9(5)	3.2(4)	135	3.0(5)	5.3(4)
140	4.8(5)	3.2(4)	140	3.4(5)	5.1(4)
145	4.2(5)	3.8(4)	145	3.0(5)	3.5(4)
150	3.3(5)	3.2(4)	150	2.4(5)	3.1(4)
155	2.7(5)	2.5(4)	155	1.9(5)	3.1(4)
160	2.3(5)	2.1(4)	160	1.6(5)	3.2(4)
165	1.9(5)	2.2(4)	165	1.4(5)	3.1(4)
170	1.7(5)	2.4(4)	170	1.2(5)	3.1(4)
175	1.5(5)	2.4(4)	175	1.0(5)	3.1(4)
180	1.3(5)	2.5(4)	180	8.8(4)	3.1(4)
185	1.2(5)	2.5(4)	185	8.0(4)	3.1(4)
190	1.1(5)	2.4(4)	190	7.4(4)	3.1(4)
195	9.6(4)	2.3(4)	195	6.7(4)	3.1(4)
200	8.7(4)	2.3(4)	200	6.3(4)	3.0(4)

Table 7-1. Day-side Electron Densities In the Peak Region (continued)

Altitude (km)	SZA = 80° - 90°		Altitude (km)	SZA = 90° - 100°	
	Average El. Dens. (cm ⁻³)	El. Dens. Std. Dev. (cm ⁻³)		Average El. Dens. (cm ⁻³)	El. Dens. Std. Dev. (cm ⁻³)
120	2.2(4)	1.0(4)	120	1.7(4)	5.8(3)
125	4.7(4)	2.6(4)	125	1.9(4)	6.7(3)
130	8.8(4)	2.5(4)	130	2.2(4)	7.5(3)
135	1.3(5)	4.3(4)	135	2.7(4)	9.8(3)
140	1.7(5)	4.2(4)	140	3.3(4)	1.4(4)
145	1.8(5)	2.8(4)	145	4.6(4)	1.7(4)
150	1.6(5)	2.0(4)	150	4.8(4)	2.1(4)
155	1.3(5)	2.1(4)	155	4.0(4)	1.8(4)
160	1.1(5)	2.1(4)	160	3.2(4)	1.6(4)
165	8.5(4)	1.8(4)	165	2.7(4)	1.4(4)
170	7.4(4)	1.6(4)	170	2.4(4)	1.3(4)
175	6.6(4)	1.4(4)	175	2.2(4)	1.1(4)
180	5.9(4)	1.3(4)	180	2.0(4)	1.1(4)
185	5.5(4)	1.3(4)	185	1.9(4)	9.4(3)
190	5.0(4)	1.2(4)	190	1.7(4)	8.4(3)
195	4.7(4)	1.1(4)	195	1.6(4)	8.0(3)
200	4.4(4)	1.0(4)	200	1.5(4)	7.6(3)

Altitude (km)	SZA = 100° - 120°	
	Average El. Dens. (cm ⁻³)	El. Dens. Std. Dev. (cm ⁻³)
120	1.6(3)	1.8(3)
125	2.5(3)	2.2(3)
130	6.9(3)	1.6(3)
135	1.7(4)	4.1(3)
140	2.5(4)	7.1(3)
145	2.9(4)	6.3(3)
150	3.0(4)	4.9(3)
155	2.8(4)	3.7(3)
160	2.1(4)	2.5(3)
165	1.8(4)	1.4(3)
170	1.6(4)	9.0(2)
175	1.4(4)	2.6(3)
180	1.3(4)	2.5(3)
185	1.2(4)	2.4(3)
190	1.1(4)	2.3(3)
195	9.8(3)	2.1(3)
200	9.1(3)	2.0(3)

Table 7-2. Average Densities, Temperatures, and Composition

Altitude (km)	Average El. Dens. (cm ⁻³)	SZA = 0° - 30°		SZA = 0° - 30°	
		El. Dens. Std. Dev. (cm ⁻³)	Average El. Temp. (K)	El. Temp. Std. Dev. (K)	Average Ion Temp. (K)
150	4.5(5)	2.0(4)	1.0(3)	1.8(2)	3.0(2)
160	2.6(5)	1.2(4)	1.2(3)	3.8(2)	0.0
170	1.8(5)	1.1(4)	1.5(3)	4.7(2)	0.0
180	1.5(5)	7.3(3)	1.9(3)	5.6(2)	0.0
190	1.2(5)	1.7(4)	2.4(3)	5.8(2)	0.0
200	9.9(4)	2.5(4)	2.8(3)	3.4(2)	6.0(2)
225	7.2(4)	1.1(4)	3.3(3)	5.8(2)	6.6(2)
250	5.7(4)	1.1(4)	3.5(3)	6.9(2)	0.1
275	4.6(4)	1.1(4)	3.6(3)	7.9(2)	1.4(3)
300	3.7(4)	6.4(3)	3.7(3)	7.3(2)	1.9(3)
350	2.8(4)	4.8(3)	3.8(3)	7.2(2)	2.7(3)
400	2.4(4)	3.2(3)	3.2(3)	4.9(2)	3.3(3)
450	2.1(4)	2.6(3)	4.2(3)	3.2(2)	3.7(3)
500	1.9(4)	1.6(3)	4.3(3)	3.4(2)	3.9(3)
600	1.7(4)	1.4(3)	4.5(3)	2.2(2)	4.2(3)
800	1.4(4)	1.5(3)	4.8(3)	3.4(2)	4.4(3)
1000	1.3(4)	1.4(3)	5.1(3)	2.3(2)	4.7(3)

Altitude (km)	Average El. Dens. (cm ⁻³)	H ⁺ Std. Dev.		Ion Composition (% of Total Mass)	
		0 ⁺ Std. Dev.	0 ⁺ Std. Dev.	0 ⁺ Std. Dev.	0 ⁺ Std. Dev.
150	4.5(5)	0.0	0.0	0.8	0.1
160	2.6(5)	0.0	0.0	2.1	0.3
170	1.8(5)	0.0	0.0	3.2	1.0
180	1.5(5)	0.0	0.0	10.0	5.3
190	1.2(5)	0.0	0.0	31.0	10.0
200	9.9(4)	0.0	0.0	57.0	8.8
225	7.2(4)	0.1	0.1	78.0	6.6
250	5.7(4)	0.2	0.1	87.0	2.5
275	4.6(4)	0.4	0.2	88.0	3.7
300	3.7(4)	0.8	0.5	87.0	4.7
350	2.8(4)	1.4	1.3	85.0	6.7
400	2.4(4)	1.5	1.0	86.0	6.2
450	2.1(4)	1.6	0.6	87.0	1.9
500	1.9(4)	1.9	0.8	85.0	2.8
600	1.7(4)	3.3	1.9	81.0	6.0
800	1.4(4)	4.0	0.7	82.0	4.8
1000	1.3(4)	4.7(3)	0.0	0.0	0.0

Table 7-2. Average Densities, Temperatures, and Composition (continued)

Altitude (km)	Average El. Dens. (cm ⁻³)	El. Dens. Std. Dev. (cm ⁻³)	Average El. Temp. (K)	El. Temp. Std. Dev. (K)	Average Ion Temp. (K)	H ⁺ Std. Dev.	H ⁺ Std. Dev.	Ion Composition (% of Total Mass)		
								O ⁺	O ²	Std. Dev.
SZA = 30° - 50°										
150	3.8(5)	2.3(4)	8.5(2)	2.5(2)	3.1(2)	0.0	0.0	1.0	0.1	0.4
160	2.5(5)	1.5(4)	1.2(3)	1.8(2)	3.9(2)	0.0	0.0	2.3	0.4	1.0
170	1.8(5)	1.8(4)	1.5(3)	2.6(2)	4.9(2)	0.0	0.0	3.6	2.0	2.6
180	1.5(5)	2.0(4)	2.0(3)	3.4(2)	5.8(2)	0.0	0.0	13.0	6.2	7.8
190	1.2(5)	2.2(4)	2.4(3)	3.0(2)	6.4(2)	0.0	0.0	35.0	9.6	11.0
200	9.8(4)	1.8(4)	2.7(3)	3.3(2)	6.2(2)	0.0	0.0	59.0	7.3	7.3
225	6.6(4)	9.3(3)	3.1(3)	5.0(2)	6.6(2)	0.1	0.1	78.0	5.7	4.4
250	5.0(4)	8.7(3)	3.3(3)	5.5(2)	9.4(2)	0.4	0.2	86.0	2.7	1.4
275	4.1(4)	8.1(3)	3.4(3)	6.9(2)	1.5(3)	0.7	0.4	88.0	2.9	1.4
300	3.4(4)	5.5(3)	3.6(3)	5.7(2)	1.9(3)	1.1	0.7	87.0	4.0	0.9
350	2.6(4)	3.9(3)	3.7(3)	3.9(2)	2.4(3)	1.7	1.6	87.0	4.7	0.5
400	2.1(4)	3.0(3)	3.9(3)	4.3(2)	2.9(3)	2.1	1.0	87.0	3.3	0.3
450	1.9(4)	2.3(3)	4.0(3)	2.8(2)	3.3(3)	3.0	2.3	85.0	5.9	0.3
500	1.7(4)	1.7(3)	4.2(3)	3.1(2)	3.6(3)	3.1	2.8	86.0	6.3	0.3
600	1.4(4)	1.2(3)	4.5(3)	3.5(2)	4.0(3)	3.3	3.2	86.0	6.1	0.1
800	1.2(4)	7.9(2)	4.8(3)	2.9(2)	4.4(3)	2.7	1.6	86.0	6.0	0.1
1000	1.0(4)	3.6(2)	5.4(3)	3.9(2)	4.7(3)	0.9	0.4	91.0	1.4	0.0

Table 7-2. Average Densities, Temperatures, and Composition (continued)

Altitude (km)	Average El. Dens. (cm ⁻³)	SZA = 50° - 70°						Ion Composition (% of Total Mass)					
		Avg. El. Dens. Std. Dev. (cm ⁻³)	Avg. El. Temp. Std. Dev. (K)	Avg. El. Temp. Std. Dev. (K)	Avg. Ion Temp. Std. Dev. (K)	H ⁺	H ⁺	H ⁺	O ⁺	O ⁺	O ⁺	O ⁺	Std. Dev.
150	1.8(4)	4.6(3)	5.0(2)	6.0(2)	2.4(2)	0.3	0.9	14.0	8.9	64.0	11.0		
160	1.2(4)	3.2(3)	1.7(3)	1.4(3)	3.3(2)	2.3	2.6	58.0	13.0	24.0	8.9		
170	9.3(3)	2.5(3)	1.8(3)	8.6(2)	5.8(2)	6.0	6.8	68.0	12.0	13.0	6.9		
180	7.3(3)	1.8(3)	2.0(3)	9.5(2)	9.3(2)	11.0	9.8	69.0	14.0	8.0	6.0		
190	5.9(3)	1.4(3)	2.2(3)	8.6(2)	1.4(3)	15.0	10.0	64.0	15.0	7.1	6.0		
200	4.7(3)	1.2(3)	2.6(3)	1.0(3)	1.9(3)	17.0	12.0	63.0	15.0	5.1	4.6		
225	3.9(3)	1.0(3)	2.6(3)	9.1(2)	3.0(3)	20.0	13.0	61.0	16.0	4.1	3.6		
250	3.6(3)	1.0(3)	2.7(3)	8.5(2)	3.6(3)	20.0	12.0	62.0	15.0	3.4	3.9		
275	3.3(3)	9.9(2)	2.8(3)	7.4(2)	4.2(3)	20.0	12.0	61.0	15.0	3.6	5.1		
300	3.1(3)	7.8(2)	3.0(3)	9.2(2)	4.8(3)	20.0	11.0	63.0	14.0	2.9	2.2		
350	2.5(3)	7.3(2)	3.2(3)	8.0(2)	5.6(3)	20.0	10.0	64.0	12.0	1.5	1.2		
400	2.1(3)	6.9(2)	3.4(3)	7.9(2)	6.4(3)	20.0	12.0	64.0	14.0	1.4	1.7		
450	1.8(3)	5.3(2)	4.0(3)	1.3(3)	7.3(3)	22.0	14.0	63.0	15.0	0.8	0.9		
500	1.5(3)	3.8(2)	4.3(3)	1.4(3)	8.2(3)	21.0	13.0	64.0	15.0	0.7	0.7		
600	1.3(3)	4.0(2)	4.4(3)	1.5(3)	9.7(3)	20.0	11.0	65.0	13.0	0.5	0.5		
800	8.9(2)	2.4(2)	5.1(3)	2.0(3)	1.4(4)	19.0	15.0	67.0	16.0	0.4	0.4		
1000	7.6(2)	1.9(2)	5.2(3)	2.1(3)	1.1(4)	22.0	18.0	63.0	18.0	0.4	0.5		

Table 7-2. Average Densities, Temperatures, and Composition (continued)

Altitude (km)	Average El. Dens. (cm ⁻³)	El. Dens. Std. Dev. (cm ⁻³)	Average El. Temp. (K)	El. Temp. Std. Dev. (K)	Average Ion Temp. (K)	H ⁺ Std. Dev.	H ⁺ Std. Dev.	Ion Composition (% of Total Mass)		
								O ⁺	0 ⁺	Std. Dev.
SZA = 70° - 80°										
150	3.3(5)	3.2(4)	9.0(2)	1.5(2)	3.1(2)	0.0	0.0	0.8	0.1	91.0
160	2.3(5)	2.1(4)	1.3(3)	2.2(2)	3.9(2)	0.0	0.0	2.3	0.3	90.0
170	1.7(5)	2.4(4)	1.7(3)	3.2(2)	5.1(2)	0.0	0.0	3.9	1.7	88.0
180	1.3(5)	2.5(4)	2.1(3)	2.6(2)	5.8(2)	0.0	0.0	6.5	6.5	72.0
190	1.1(5)	2.4(4)	2.4(3)	2.8(2)	6.0(2)	0.0	0.0	40.0	8.6	44.0
200	8.7(4)	2.3(4)	2.7(3)	2.8(2)	6.0(2)	0.1	0.0	61.0	6.9	22.0
225	6.0(4)	6.5(3)	3.0(3)	3.2(2)	6.7(2)	0.2	0.2	78.0	5.7	7.7
250	4.6(4)	5.4(3)	3.1(3)	3.2(2)	9.2(2)	0.5	0.3	86.0	2.5	2.5
275	3.7(4)	4.3(3)	3.2(3)	3.2(2)	1.4(3)	0.9	0.6	88.0	2.5	1.7
300	3.1(4)	3.5(3)	3.5(3)	3.4(2)	1.7(3)	1.4	1.0	88.0	2.7	1.2
350	2.3(4)	3.0(3)	3.8(3)	4.1(2)	2.0(3)	2.0	1.3	87.0	3.2	0.9
400	1.9(4)	2.5(3)	3.9(3)	3.4(2)	2.4(3)	2.5	1.5	87.0	3.3	0.6
450	1.6(4)	2.1(3)	4.2(3)	4.3(2)	2.6(3)	2.9	1.6	86.0	4.3	0.5
500	1.4(4)	1.7(3)	4.3(3)	3.2(2)	2.7(3)	3.4	2.2	85.0	5.0	0.4
600	1.2(4)	1.2(3)	4.5(3)	3.4(2)	2.8(3)	4.1	2.8	86.0	5.4	0.3
800	1.0(4)	7.5(2)	4.8(3)	3.1(2)	3.0(3)	4.9	3.1	86.0	4.9	0.2
1000	8.2(3)	4.8(2)	5.1(3)	2.8(2)	2.9(3)	4.3	1.7	87.0	3.3	0.1

Table 7-2. Average Densities, Temperatures, and Composition (continued)

Altitude (km)	Average El. Dens. (cm ⁻³)	El. Dens. Std. Dev. (cm ⁻³)	Average El. Temp. (K)	El. Temp. Std. Dev. (K)	Average Ion Temp. (K)	H ⁺ Std. Dev.	H ⁺ Std. Dev.	Ion Composition (% of Total Mass)		
								O ⁺	O ₂	O ₂ Std. Dev.
SZA = 80° - 90°										
150	2.4(5)	3.1(4)	1.0(3)	1.6(2)	3.2(2)	0.0	0.0	1.2	0.4	91.0
160	1.6(5)	3.2(4)	1.3(3)	1.9(2)	4.3(2)	0.0	0.0	2.5	0.6	90.0
170	1.2(5)	3.1(4)	1.7(3)	3.4(2)	5.3(2)	0.0	0.0	5.7	3.4	85.0
180	8.8(4)	3.1(4)	2.2(3)	3.3(2)	6.0(2)	0.0	0.0	25.0	9.8	11.0
190	7.4(4)	3.1(4)	2.5(3)	2.9(2)	6.4(2)	0.1	0.0	46.0	9.8	36.0
200	6.3(4)	3.0(4)	2.7(3)	3.2(2)	6.6(2)	0.2	0.1	64.0	6.5	19.0
225	4.7(4)	5.9(3)	3.0(3)	2.5(2)	8.4(2)	0.4	0.3	77.0	6.3	8.9
250	3.7(4)	4.4(3)	3.2(3)	2.6(2)	1.1(3)	0.8	0.6	85.0	3.8	4.0
275	3.0(4)	2.9(3)	3.3(3)	2.7(2)	1.3(3)	1.4	1.0	85.0	4.6	3.3
300	2.6(4)	2.6(3)	3.5(3)	2.9(2)	1.5(3)	1.9	1.5	86.0	3.6	2.4
350	2.0(4)	2.6(3)	3.7(3)	3.1(2)	1.8(3)	2.9	2.1	86.0	3.8	1.7
400	1.6(4)	2.1(3)	3.9(3)	3.4(2)	2.0(3)	3.2	2.3	86.0	4.5	1.2
450	1.4(4)	1.9(3)	4.1(3)	3.0(2)	2.1(3)	3.4	2.3	87.0	4.1	0.8
500	1.2(4)	1.6(3)	4.3(3)	3.5(2)	2.2(3)	3.7	2.8	86.0	5.5	0.7
600	9.9(3)	1.2(3)	4.5(3)	3.2(2)	2.3(3)	4.3	2.9	86.0	5.7	0.6
800	8.0(3)	7.1(2)	4.8(3)	4.2(2)	2.5(3)	4.7	2.4	85.0	4.0	0.2
1000	6.3(3)	5.1(2)	5.1(3)	5.3(2)	2.8(3)	5.1	3.1	85.0	4.6	0.1

Table 7-2. Average Densities, Temperatures, and Composition (continued)

Altitude (km)	Average El. Dens. (cm ⁻³)	El. Dens. Std. Dev. (cm ⁻³)	Average El. Temp. (K)	El. Temp. Std. Dev. (K)	Average Ion Temp. (K)	H ⁺ Std. Dev.	H ⁺ Std. Dev.	Ion Composition (% of Total Mass)			O ₂ Std. Dev.
								O ₂ Std. Dev.	O ₂ Std. Dev.	O ₂ Std. Dev.	
SZA = 90° - 100°											
150	1.6(5)	2.0(4)	8.0(2)	2.1(2)	2.9(2)	0.0	0.0	1.4	0.3	89.0	1.9
160	1.1(5)	2.1(4)	1.5(3)	2.8(2)	4.4(2)	0.0	0.0	3.6	1.5	88.0	3.1
170	7.4(4)	1.6(4)	1.8(3)	3.5(2)	5.3(2)	0.0	0.0	13.0	10.0	73.0	13.0
180	5.9(4)	1.3(4)	2.3(3)	2.9(2)	5.8(2)	0.1	0.2	38.0	14.0	44.0	14.0
190	5.0(4)	1.2(4)	2.4(3)	4.2(2)	6.4(2)	0.3	0.4	57.0	10.0	25.0	9.1
200	4.4(4)	1.0(4)	2.5(3)	3.3(2)	7.5(2)	0.5	0.6	67.0	8.0	16.0	6.7
225	3.3(4)	5.2(3)	2.8(3)	2.9(2)	1.1(3)	1.1	1.3	76.0	8.3	10.0	6.2
250	2.6(4)	4.1(3)	3.0(3)	2.5(2)	1.3(3)	1.9	2.3	81.0	7.1	6.2	4.9
275	2.1(4)	3.0(3)	3.1(3)	2.3(2)	1.4(3)	2.3	2.3	82.0	6.9	5.1	4.1
300	1.8(4)	2.6(3)	3.3(3)	3.1(2)	1.5(3)	3.2	3.0	83.0	6.3	3.6	2.7
350	1.4(4)	2.8(3)	3.6(3)	5.6(2)	1.7(3)	4.1	3.5	84.0	5.8	2.5	1.8
400	1.2(4)	2.0(3)	3.8(3)	3.8(2)	1.8(3)	4.1	3.3	84.0	7.8	2.0	2.3
450	1.0(4)	1.6(3)	4.0(3)	4.4(2)	1.9(3)	4.9	3.9	85.0	6.4	1.3	1.4
500	9.3(3)	1.3(3)	4.3(3)	4.3(2)	2.0(3)	4.8	3.7	85.0	6.4	1.1	1.5
600	8.0(3)	1.1(3)	4.6(3)	5.1(2)	2.0(3)	5.6	4.5	85.0	6.3	0.7	1.6
800	6.2(3)	8.1(2)	4.8(3)	5.0(2)	2.3(3)	6.7	5.6	84.0	7.6	0.5	1.1
1000	5.0(3)	4.3(2)	5.1(3)	8.8(2)	2.5(3)	6.8	5.2	84.0	7.1	0.5	0.6

Table 7-2. Average Densities, Temperatures, and Composition (continued)

Altitude (km)	Average El. Dens. (cm ⁻³)	El. Dens. Std. Dev. (cm ⁻³)	Average El. Temp. (K)	El. Temp. Std. Dev. (K)	Average Ion Temp. (K)	H ⁺ Std. Dev.	Ion Composition (% of Total Mass)		
							H ⁺	O ⁺	0 ⁺
SZA = 100° - 120°									
150	4.8(4)	2.1(4)	7.2(2)	3.0(2)	2.3(2)	0.0	0.0	4.1	86.0
160	3.2(4)	1.6(4)	1.4(3)	4.5(2)	4.1(2)	0.2	0.3	28.0	16.0
170	2.4(4)	1.3(4)	1.7(3)	4.4(2)	6.0(2)	1.0	1.7	53.0	18.0
180	2.0(4)	1.1(4)	2.1(3)	4.3(2)	8.0(2)	2.1	3.0	71.0	29.0
190	1.7(4)	8.4(3)	2.3(3)	4.6(2)	1.1(3)	3.2	4.1	75.0	11.0
200	1.5(4)	7.6(3)	2.6(3)	4.7(2)	1.3(3)	4.5	5.3	76.0	11.0
225	1.2(4)	2.7(3)	2.9(3)	7.2(2)	1.5(3)	6.7	7.5	75.0	12.0
250	9.9(3)	2.4(3)	3.2(3)	7.4(2)	1.7(3)	7.5	7.9	76.0	12.0
275	8.7(3)	2.1(3)	3.4(3)	7.6(2)	1.7(3)	8.4	8.9	77.0	12.0
300	7.9(3)	1.9(3)	3.6(3)	6.3(2)	1.8(3)	9.3	8.9	76.0	13.0
350	6.8(3)	2.0(3)	3.7(3)	7.0(2)	1.8(3)	9.2	8.3	77.0	13.0
400	5.9(3)	1.3(3)	3.9(3)	4.5(2)	1.9(3)	9.0	7.9	79.0	12.0
450	5.3(3)	1.0(3)	4.1(3)	6.5(2)	1.9(3)	8.9	7.8	79.0	11.0
500	4.8(3)	9.6(2)	4.4(3)	6.2(2)	2.0(3)	9.1	8.1	81.0	9.0
600	4.0(3)	8.2(2)	4.9(3)	9.7(2)	2.0(3)	8.3	7.3	81.0	9.3
800	3.2(3)	8.1(2)	5.2(3)	9.4(2)	2.2(3)	8.9	6.9	82.0	7.6
1000	2.7(3)	5.0(2)	7.9(2)	2.2(3)	7.1	7.1	7.1	81.0	8.6

Table 7-2. Average Densities, Temperatures, and Composition (continued)

Altitude (km)	Average El. Dens. (cm ⁻³)	El. Dens. Std. Dev. (cm ⁻³)	Average El. Temp. (K)	El. Temp. Std. Dev. (K)	Average Ion Temp. (K)	H ⁺ Std. Dev.	SZA = 120° - 150°			SZA = 150° - 180°		
							H ⁺ Std. Dev.	0 ⁺ Std. Dev.	Ion Composition (% of Total Mass) 0 ⁺	H ⁺ Std. Dev.	0 ⁺ Std. Dev.	Ion Composition (% of Total Mass) 0 ⁺
150	3.0(4)	4.9(3)	6.5(2)	3.2(2)	2.1(2)	0.0	0.1	8.4	0.2	71.0	15.0	
160	2.1(4)	2.5(3)	1.4(3)	3.7(2)	3.1(2)	2.0	2.0	47.0	0.5	32.0	14.0	
170	1.6(4)	9.0(2)	1.6(3)	4.2(2)	5.4(2)	6.2	5.7	64.0	0.5	16.0	8.3	
180	1.3(4)	2.5(3)	2.0(3)	6.0(2)	9.1(2)	13.0	11.0	68.0	0.5	7.5	3.8	
190	1.1(4)	2.3(3)	2.3(3)	5.2(2)	1.5(3)	17.0	14.0	68.0	0.4	4.5	2.2	
200	9.1(3)	2.0(3)	2.5(3)	4.7(2)	2.0(3)	21.0	16.0	65.0	0.4	3.6	2.2	
225	7.1(3)	1.2(3)	2.8(3)	5.9(2)	2.4(3)	25.0	19.0	61.0	0.6	2.8	2.3	
250	6.2(3)	1.0(3)	3.1(3)	5.9(2)	2.7(3)	30.0	20.0	58.0	1.1	1.9	1.6	
275	5.4(3)	9.8(2)	3.1(3)	5.9(2)	2.6(3)	28.0	20.0	59.0	1.4	1.4	1.2	
300	4.9(3)	7.8(2)	3.3(3)	6.2(2)	2.5(3)	30.0	20.0	58.0	0.8	1.4	2.0	
350	4.0(3)	8.8(2)	3.6(3)	9.9(2)	2.4(3)	25.0	19.0	64.0	0.8	1.0	1.0	
400	3.3(3)	7.0(2)	4.0(3)	1.2(3)	2.3(3)	30.0	19.0	59.0	0.8	1.3	3.0	
450	2.8(3)	6.3(2)	4.1(3)	1.0(3)	2.3(3)	27.0	19.0	61.0	1.5	1.4	3.8	
500	2.4(3)	5.2(2)	4.4(3)	1.2(3)	2.2(3)	25.0	18.0	65.0	1.7	0.7	1.9	
600	2.0(3)	3.9(2)	4.8(3)	1.1(3)	2.2(3)	23.0	18.0	66.0	1.4	0.9	2.6	
800	1.5(3)	3.4(2)	5.5(3)	1.2(3)	2.6(3)	22.0	17.0	68.0	1.7	1.0	4.3	
1000	1.3(3)	2.8(2)	5.7(3)	1.1(3)	2.8(3)	22.0	14.0	69.0	0.5	0.5	1.2	

Table 7-2. Average Densities, Temperatures, and Composition (continued)

Altitude (km)	Average El. Dens. (cm ⁻³)	El. Dens. Std. Dev. (cm ⁻³)	Average El. Temp. (K)	El. Temp. Std. Dev. (K)	SZA = 150° - 170°		Ion Composition (% of Total Mass)		O ₂ Std. Dev.
					H ⁺	Std. Dev.	H ⁺	Std. Dev.	
150	2.6(4)	5.3(3)	5.1(2)	3.2(2)	2.3(2)	0.0	15.0	9.8	70.0
160	1.5(4)	4.4(3)	1.3(3)	5.9(2)	3.5(2)	3.5	55.0	12.0	24.0
170	1.1(4)	3.0(3)	1.8(3)	8.3(2)	5.0(2)	9.0	63.0	14.0	13.0
180	7.8(3)	2.3(3)	2.0(3)	7.2(2)	8.0(2)	17.0	63.0	18.0	6.8
190	6.5(3)	1.7(3)	2.2(3)	7.4(2)	1.2(3)	23.0	18.0	59.0	21.0
200	5.7(3)	1.4(3)	2.4(3)	7.6(2)	1.7(3)	26.0	20.0	56.0	21.0
225	4.6(3)	1.2(3)	2.7(3)	7.2(2)	2.8(3)	28.0	21.0	56.0	21.0
250	4.1(3)	9.9(2)	2.9(3)	7.5(2)	3.5(3)	29.0	21.0	56.0	21.0
275	3.6(3)	9.5(2)	3.1(3)	1.0(3)	4.1(3)	25.0	19.0	60.0	19.0
300	3.3(3)	8.7(2)	3.3(3)	8.0(2)	4.7(3)	28.0	20.0	58.0	20.0
350	2.7(3)	7.4(2)	3.5(3)	8.7(2)	5.5(3)	25.0	19.0	62.0	20.0
400	2.3(3)	6.3(2)	3.7(3)	1.0(3)	6.1(3)	25.0	18.0	63.0	18.0
450	2.0(3)	5.5(2)	3.9(3)	1.1(3)	6.5(3)	24.0	18.0	63.0	19.0
500	1.8(3)	4.5(2)	4.1(3)	1.1(3)	6.7(3)	21.0	17.0	67.0	18.0
600	1.5(3)	3.8(2)	4.5(3)	1.3(3)	7.1(3)	23.0	18.0	64.0	19.0
800	1.1(3)	2.8(2)	5.1(3)	1.5(3)	8.4(3)	23.0	17.0	65.0	18.0
1,000	9.5(2)	2.4(2)	5.4(3)	1.8(3)	9.4(3)	26.0	19.0	62.0	21.0

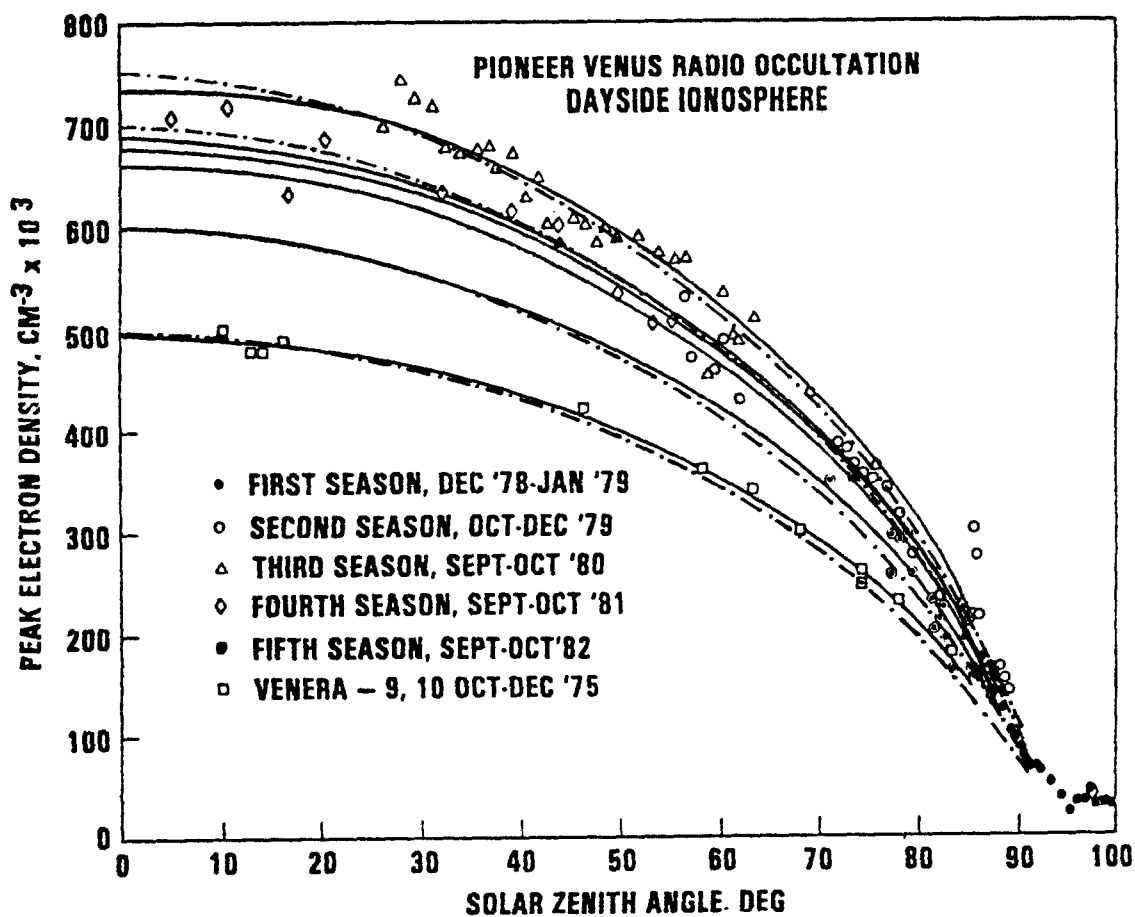


Figure 7-1. Peak Electron Densities vs. Solar Zenith Angle for Various Times of Measurement. Differences reflect the influence of solar cycle effects (from Kliore, 1984).

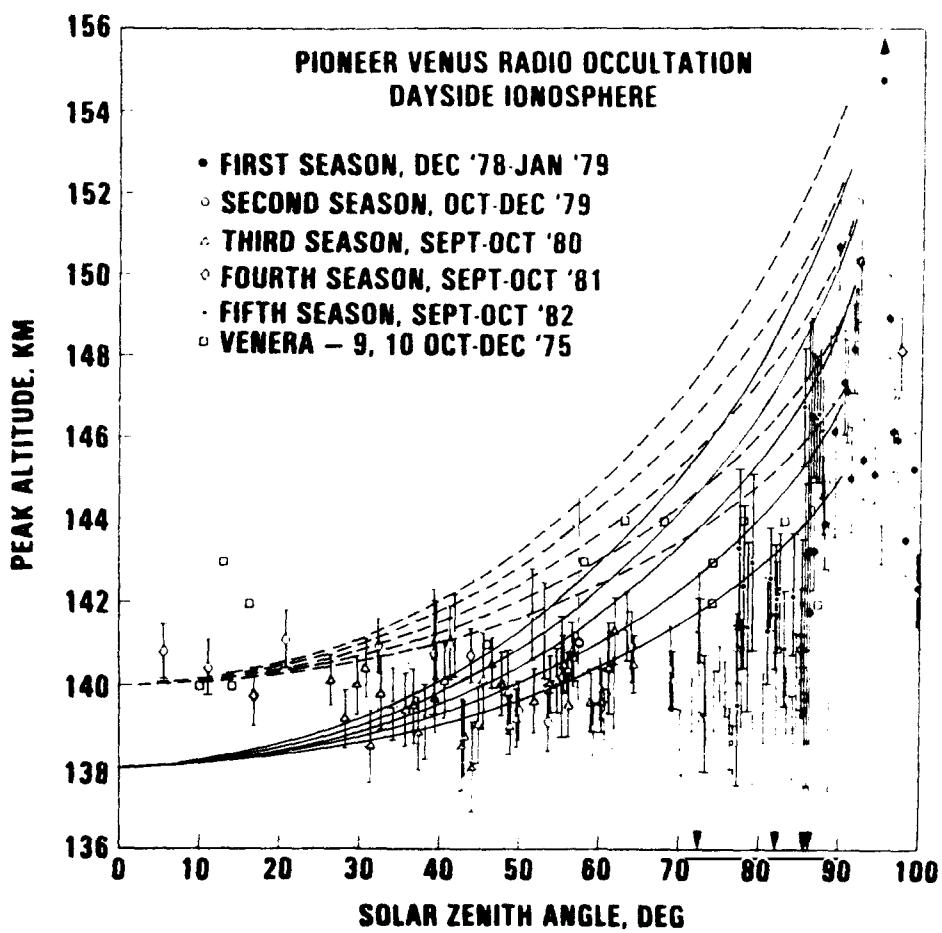


Figure 7-2. Peak Altitude vs. Solar Zenith Angle for the Data Shown in Figure 7-1

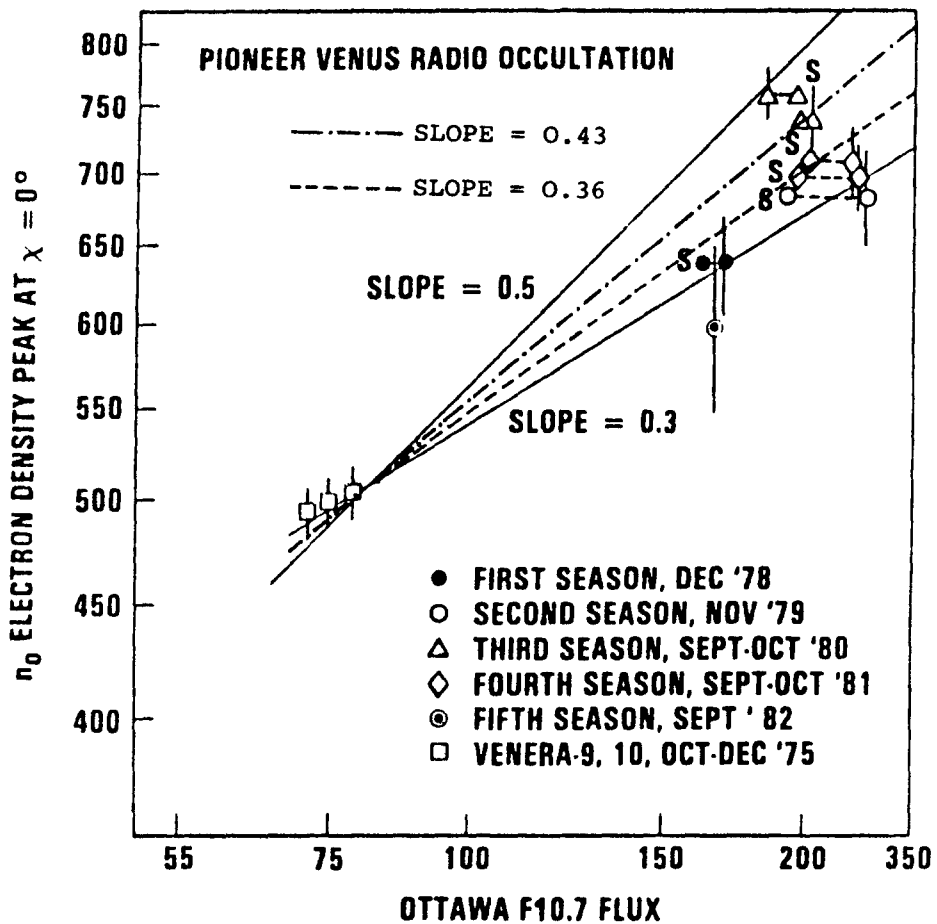


Figure 7-3. Dependence of Averaged Sub-Solar ($\chi = 0^\circ$) Peak Electron Densities on Solar Flux, as Represented by the F10.7 Index. A slope of $m = 0.36$ gives the best fit (see text).

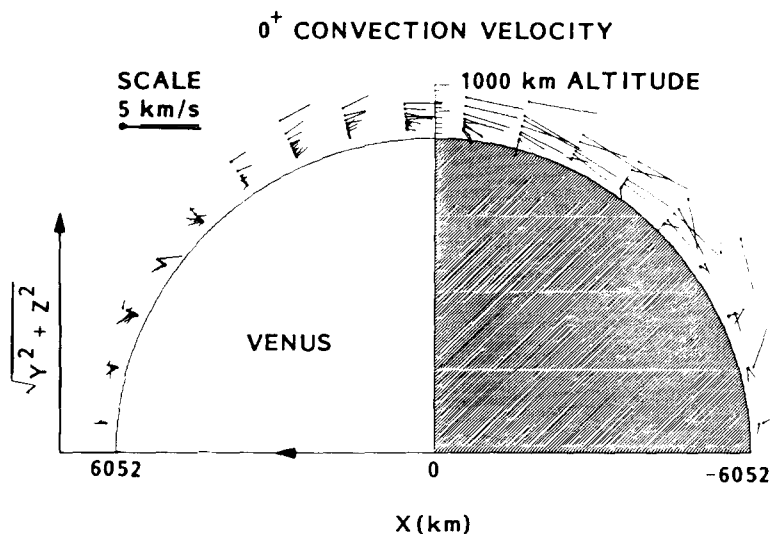


Figure 7-4. O^+ Velocities as Measured by the Pioneer Venus ORPA (Miller *et al.*, 1984)

**PIONEER VENUS OCCULTATION
VENUS NIGHTSIDE IONOSPHERE PEAK**

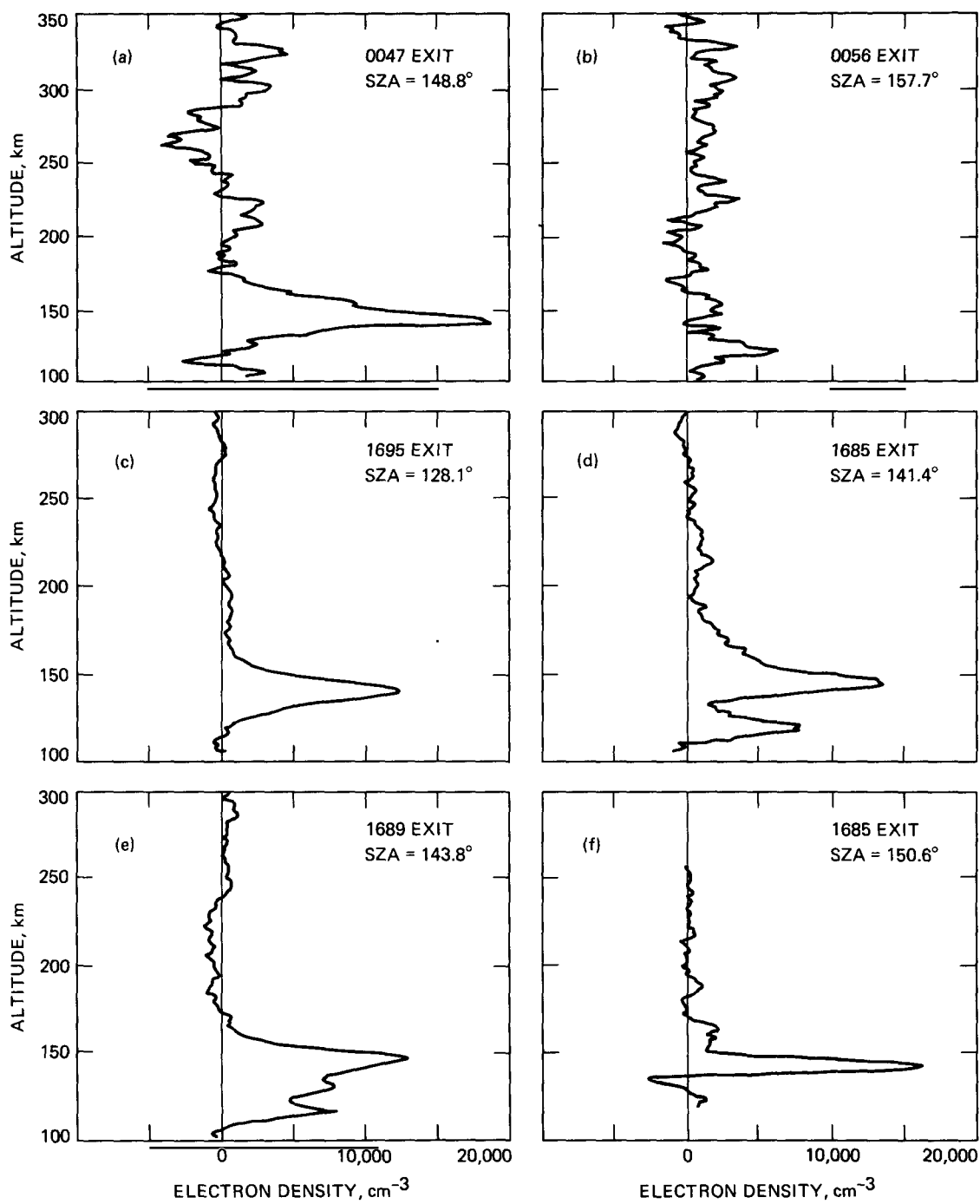


Figure 7-5. Representative Profiles of Ionization in the Peak Region of the Nightside Ionosphere (from Kliore, 1984)

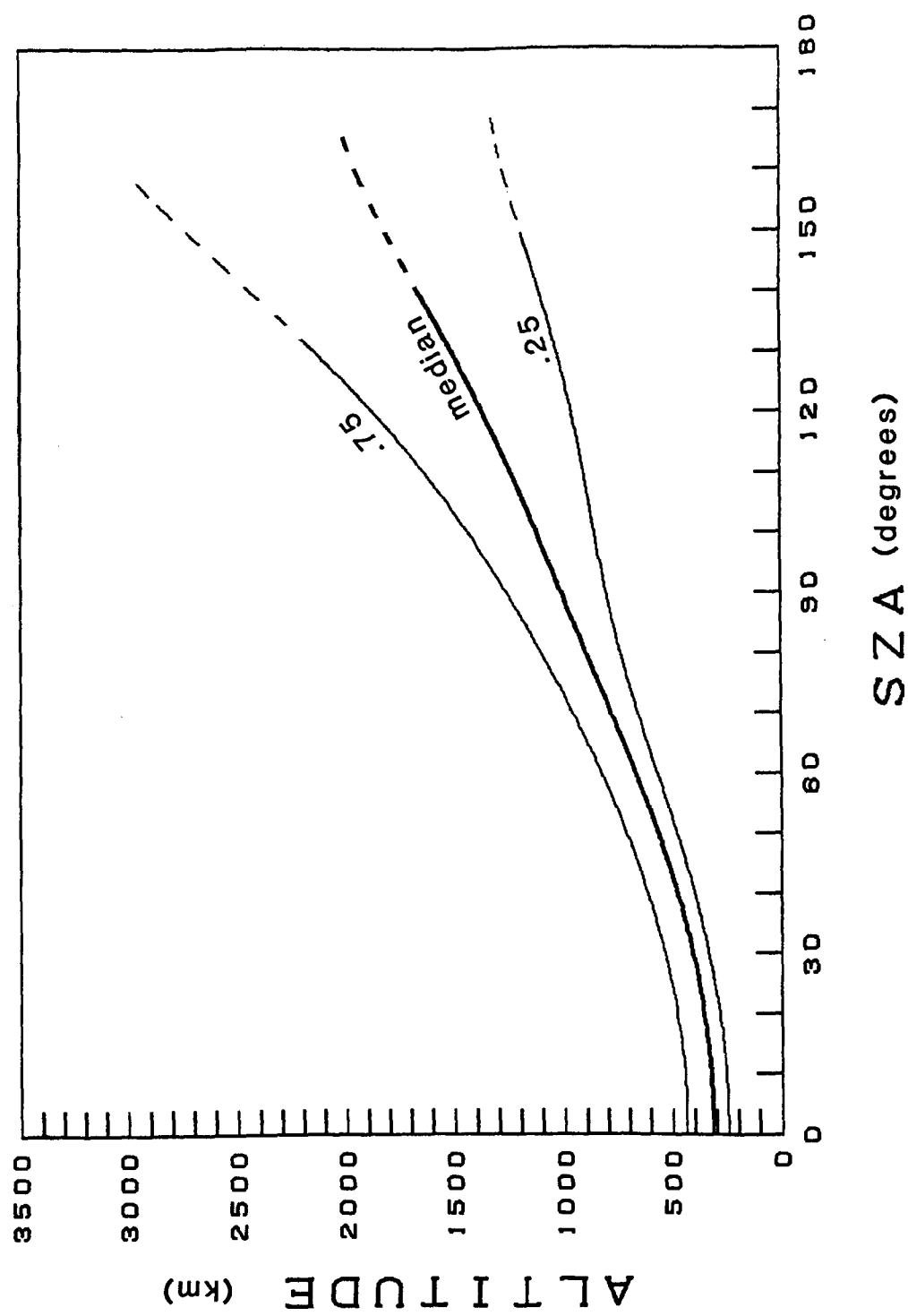


Figure 7-6. Behavior of the Ionopause With Solar Zenith Angle (from Brace, 1984)

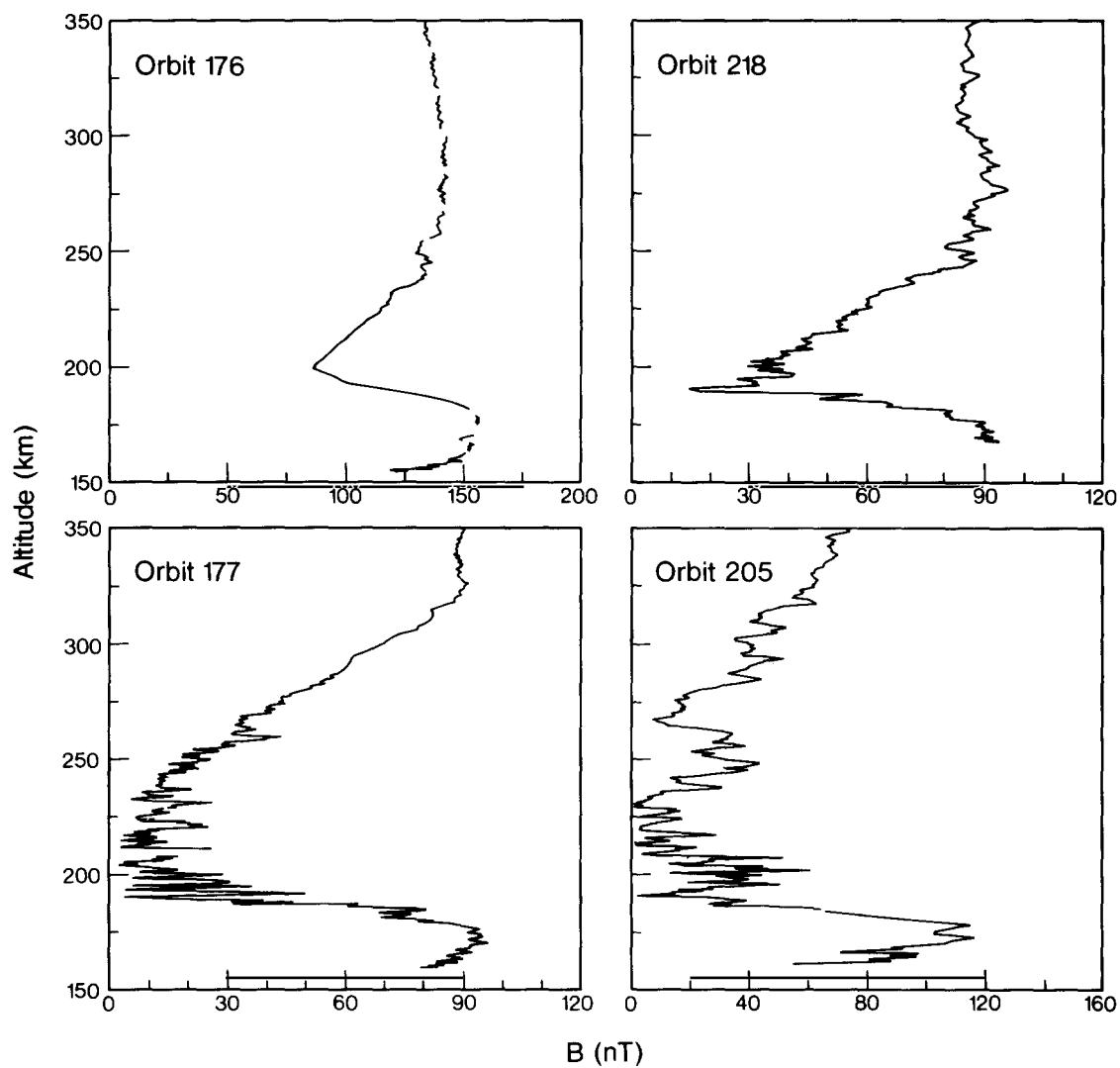


Figure 7-7. Magnetic Field Strength in the Low-Altitude Ionosphere for Several Instances of Low Solar Zenith Angles and High Solar Wind Dynamic Pressures (Russell and Vaisberg, 1983)

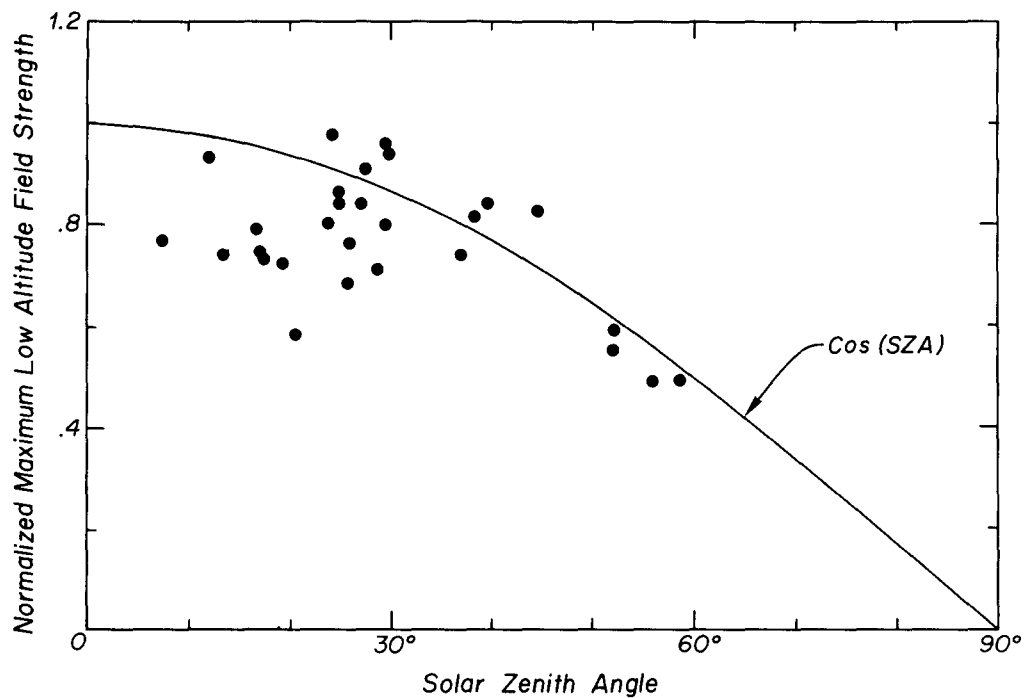


Figure 7-8. Solar Zenith Angle Dependence of Low-Altitude Magnetic Field Strength (Russell and Vaisberg, 1983)

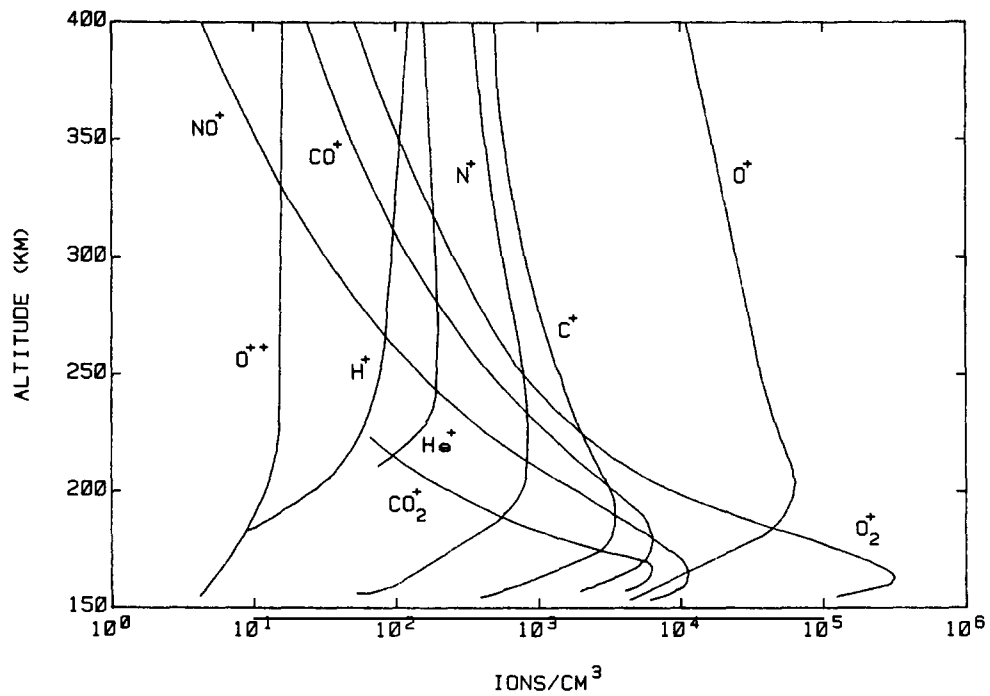


Figure 7-9. An Example of Ion Densities for Species Observed with the Pioneer Venus IMS (Taylor, Jr. et al., 1979)

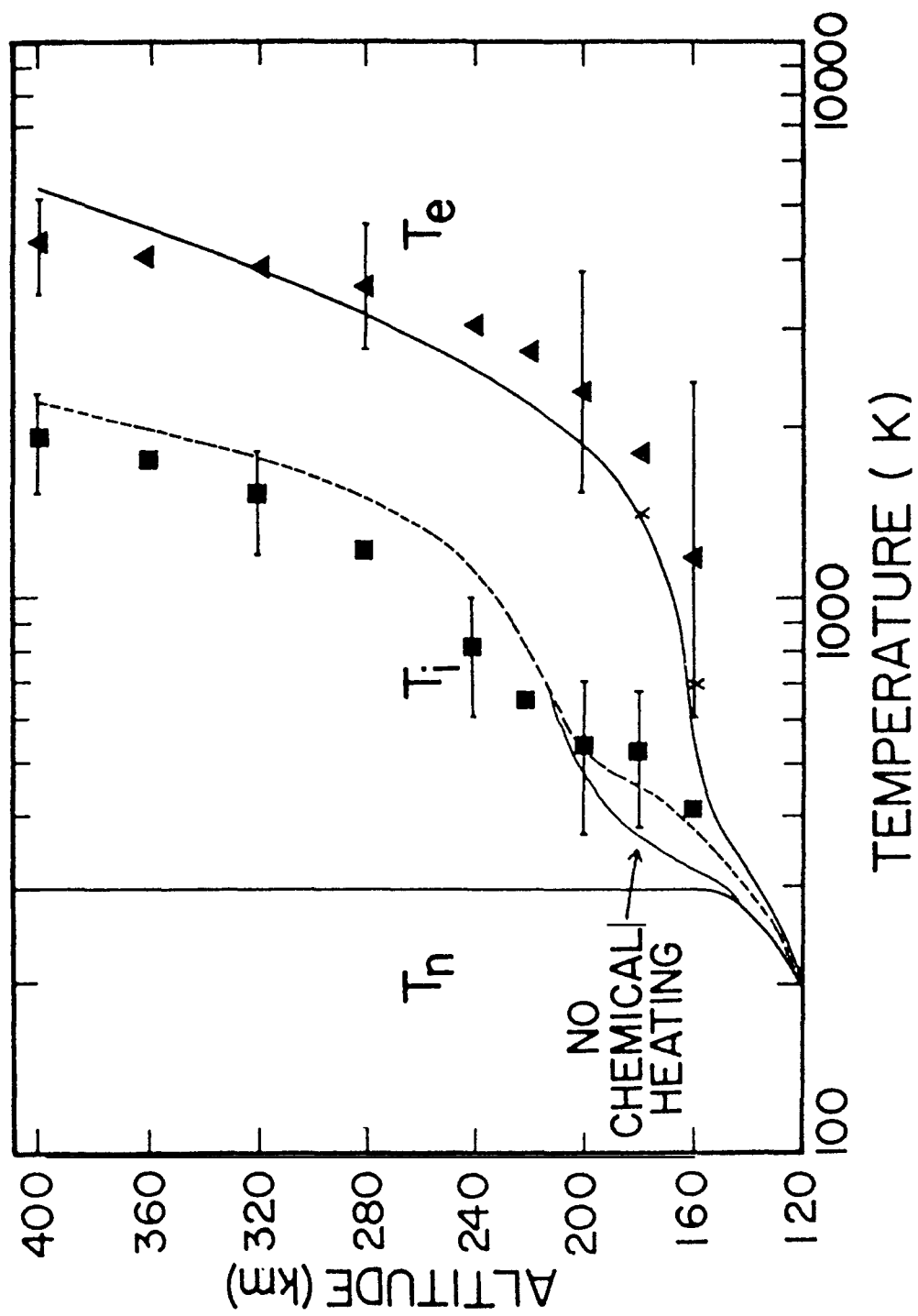


Figure 7-10. Electron and Ion Temperatures in the Ionosphere (Knudsen et al., 1979; Nagy et al., 1979; Cravens et al., 1980)

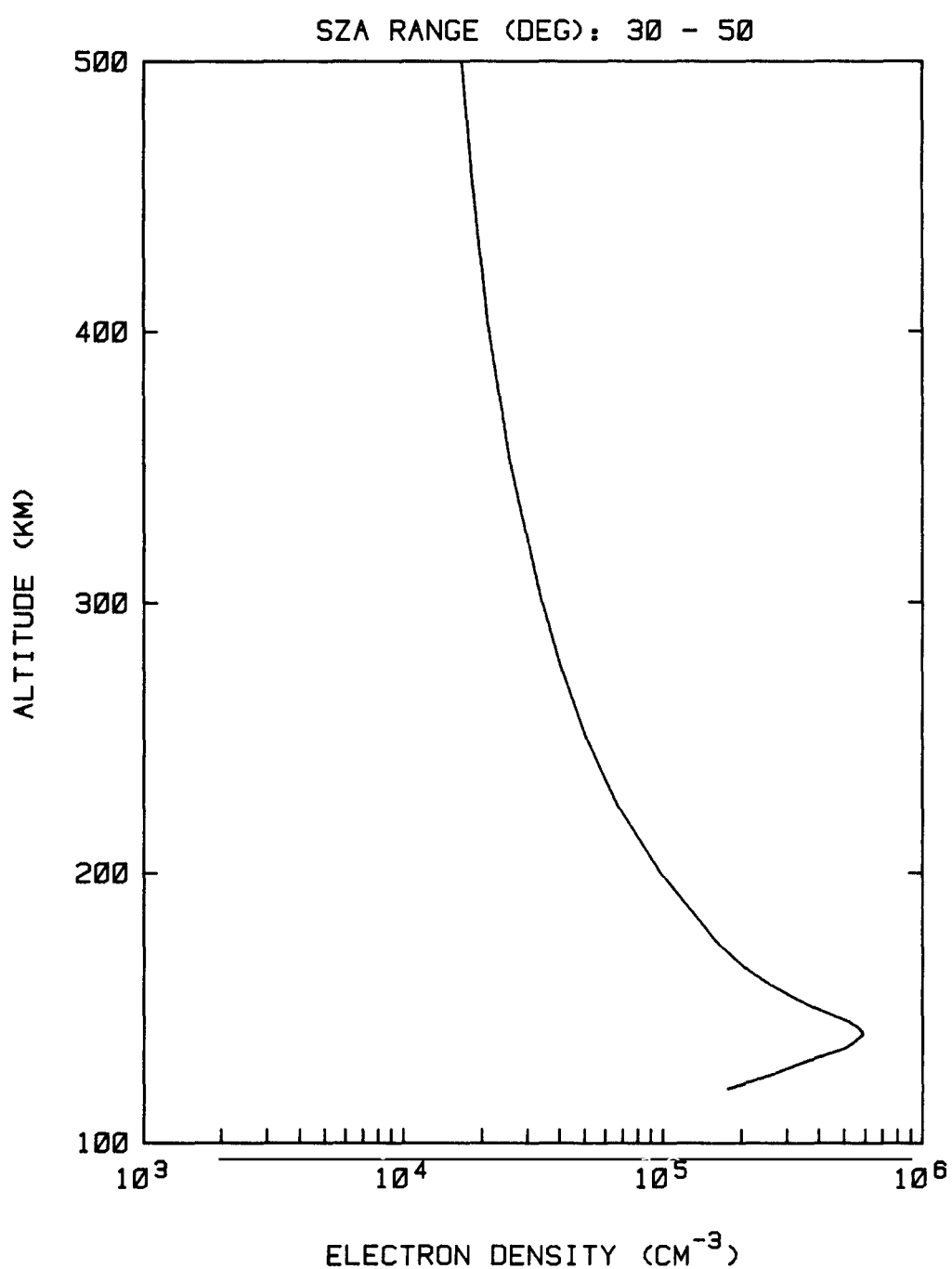


Figure 7-11. VIRA Model Ionosphere - Electron Density vs. Altitude, $30^\circ < \text{SZA} < 50^\circ$

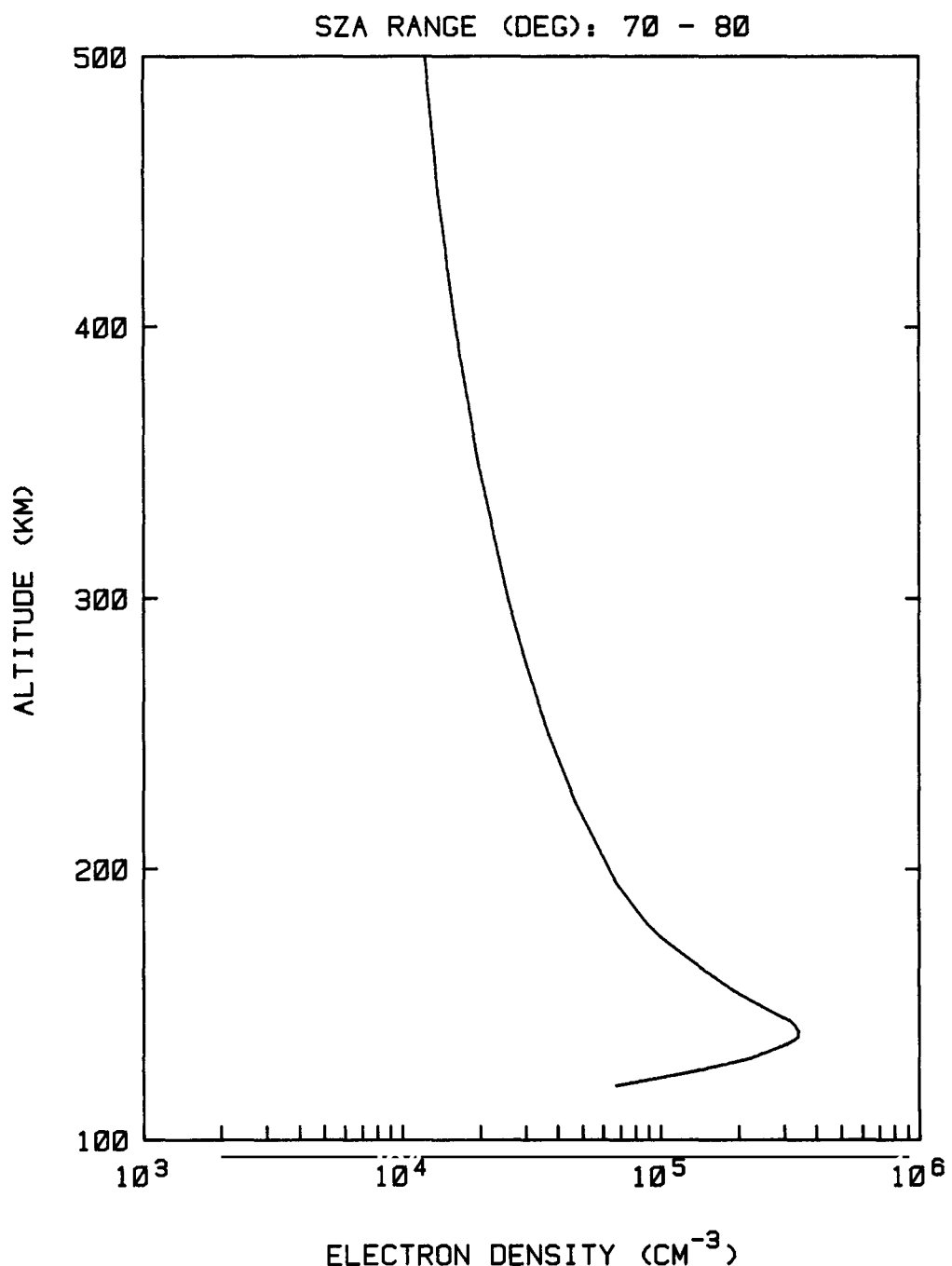


Figure 7-12. VIRA Model Ionosphere - Electron Density vs. Altitude, $70^\circ < \text{SZA} < 80^\circ$

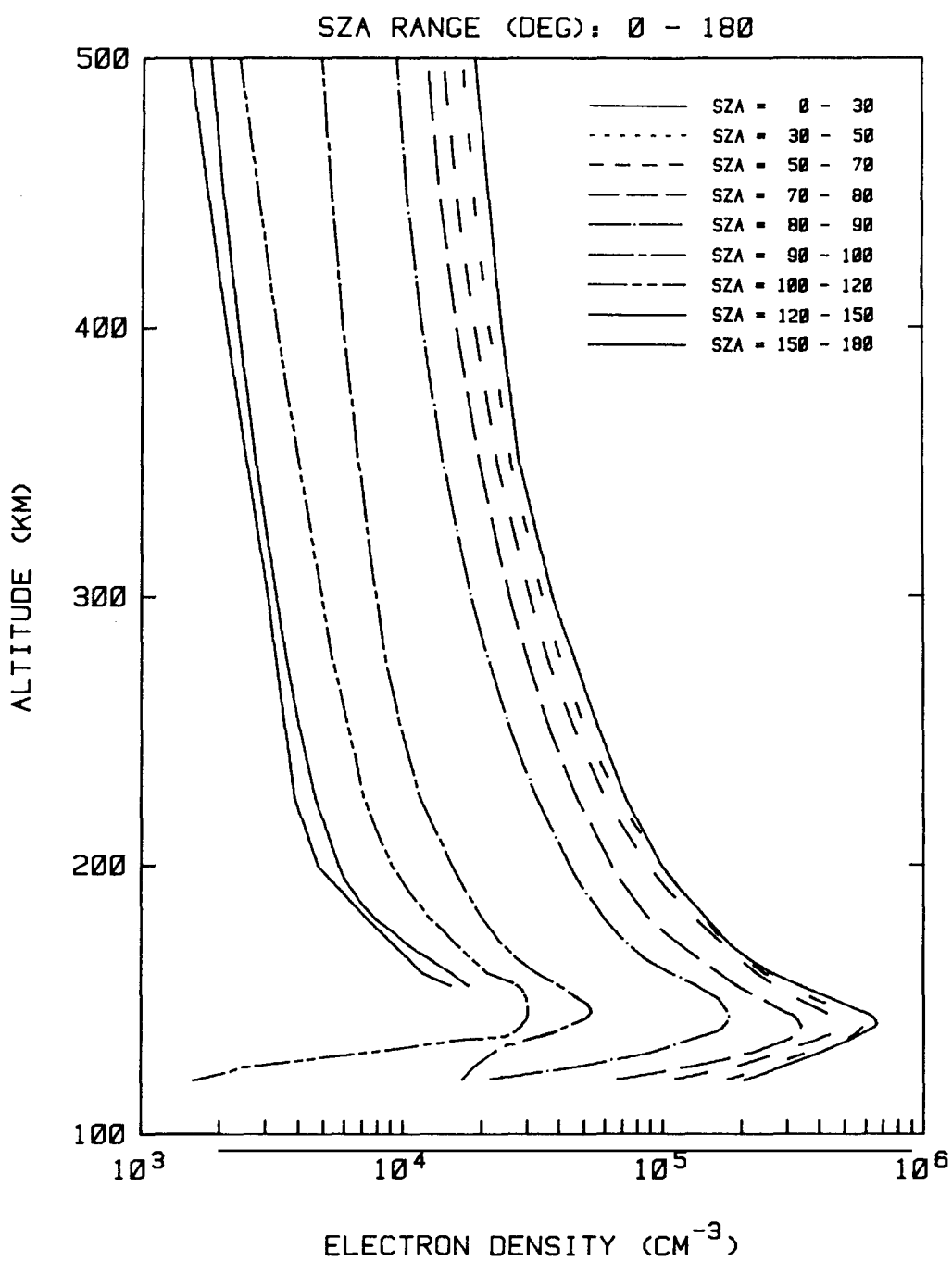


Figure 7-13. VIRA Model Ionosphere - Electron Profiles for All Solar Zenith Angle Ranges in Table 7-2

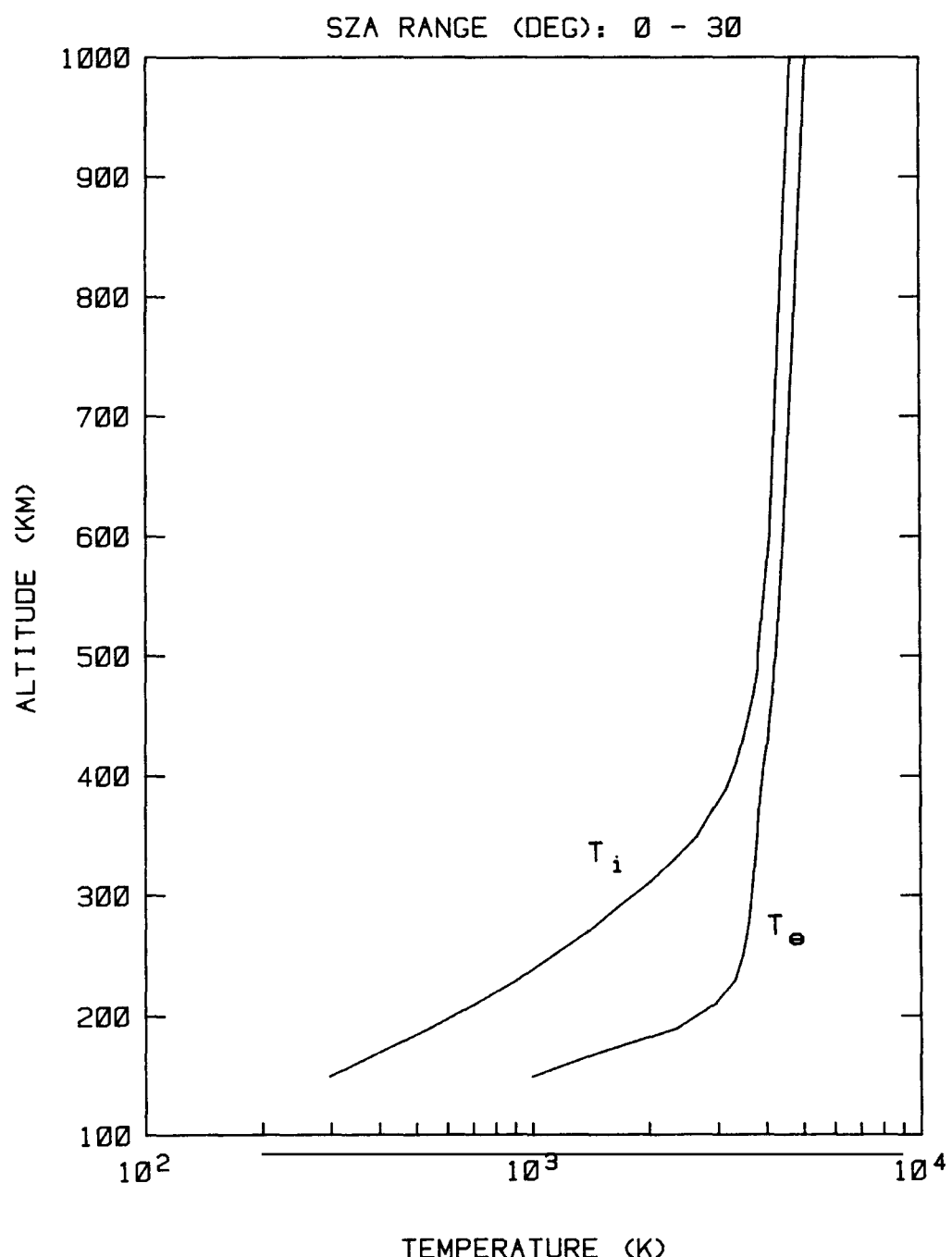


Figure 7-14. VIRA Model Ionosphere - Ion and Electron Temperatures, $0^\circ < \text{SZA} < 30^\circ$

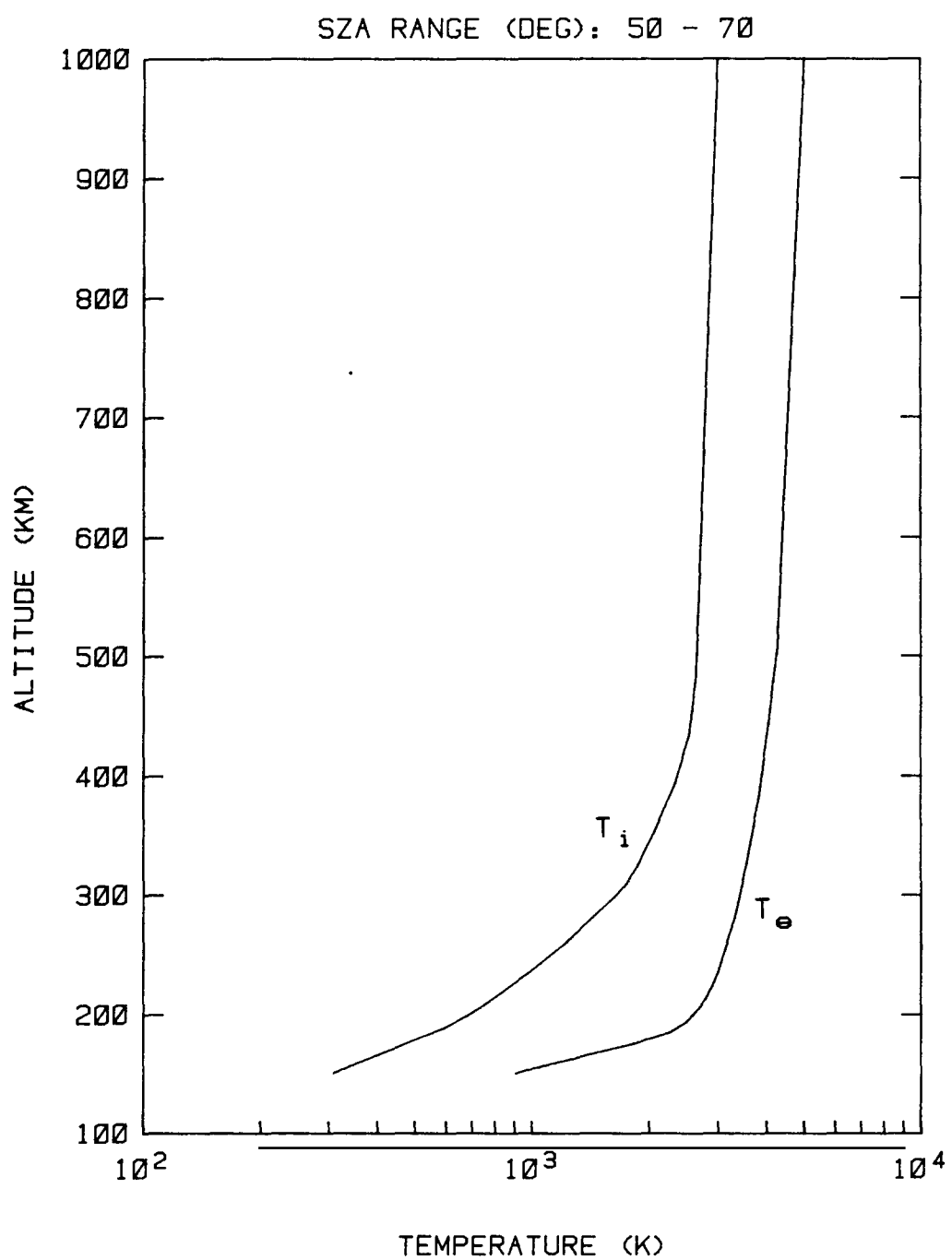


Figure 7-15. VIRA Model Ionosphere - Ion and Electron Temperatures, $50^\circ < \text{SZA} < 70^\circ$

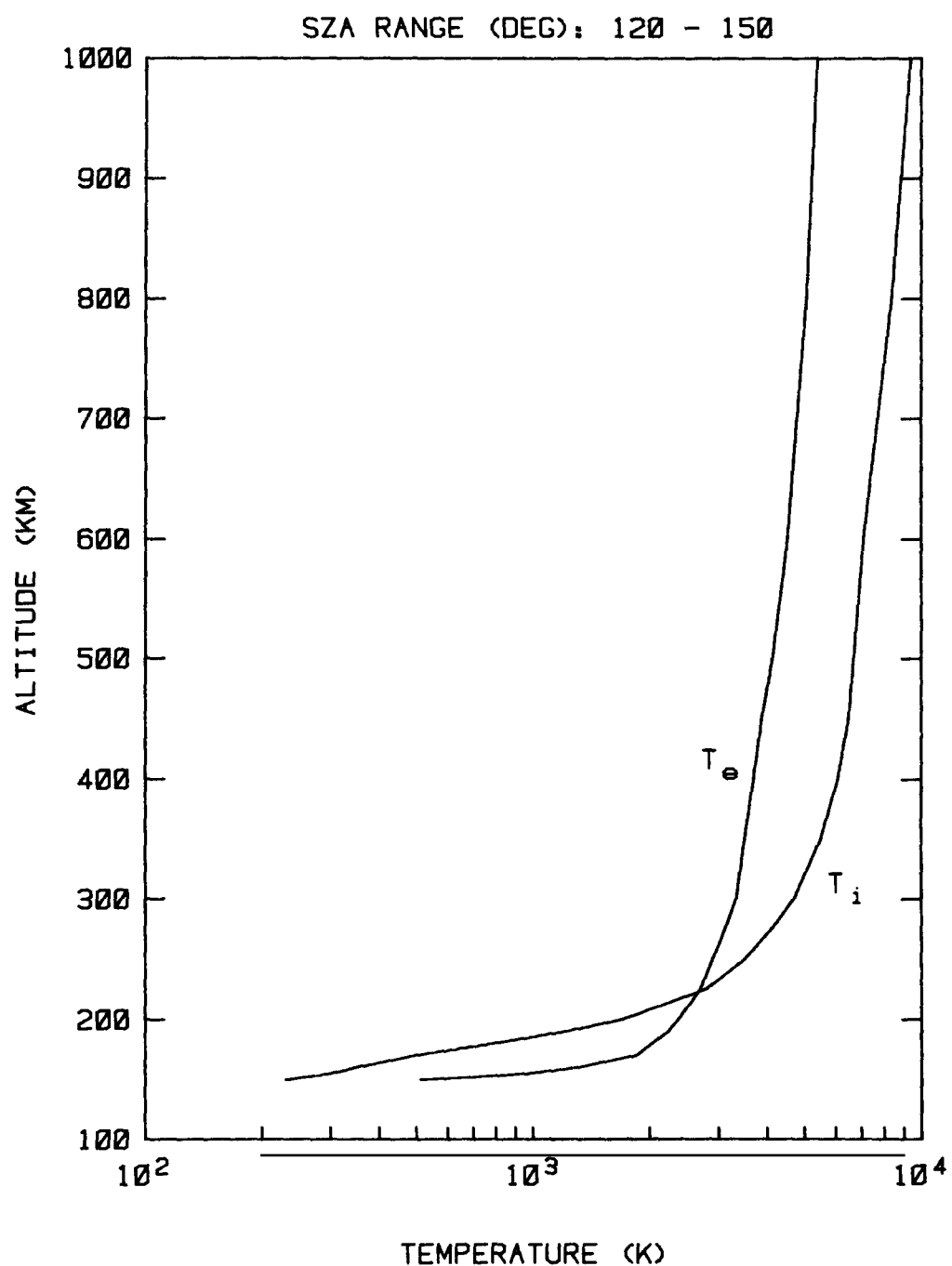


Figure 7-16. VIRA Model Ionosphere - Ion and Electron Temperatures, $120^\circ < \text{SZA} < 150^\circ$

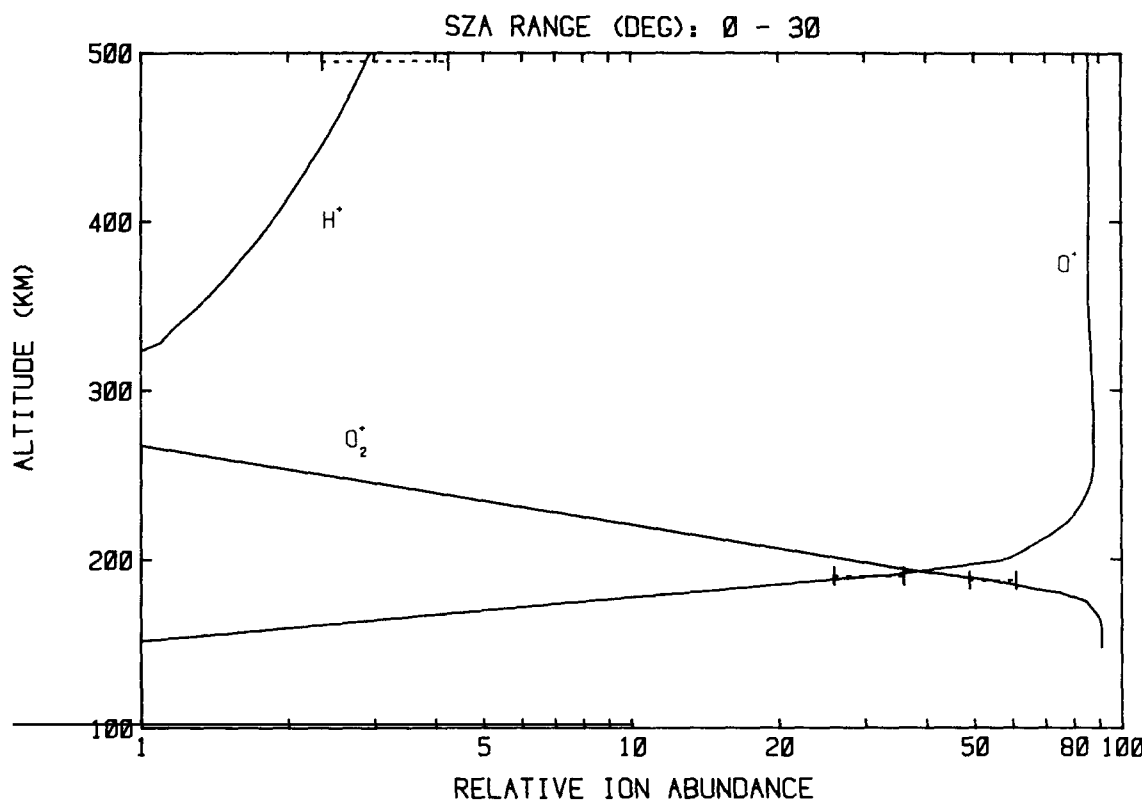


Figure 7-17. VIRA Model Ionosphere - Relative Abundances of H^+ , O^+ , and O_2^+ , $0^\circ < \text{SZA} < 30^\circ$

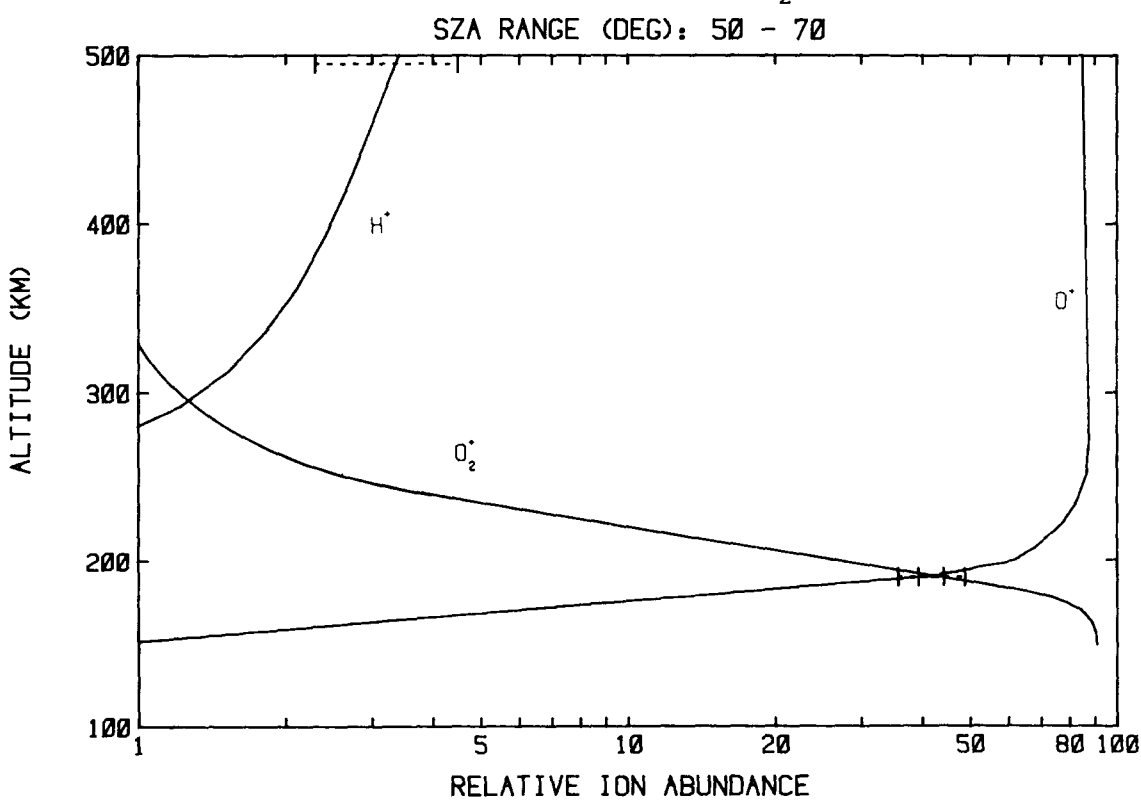


Figure 7-18. VIRA Model Ionosphere - Relative Abundances of H^+ , O^+ , and O_2^+ , $50^\circ < \text{SZA} < 70^\circ$

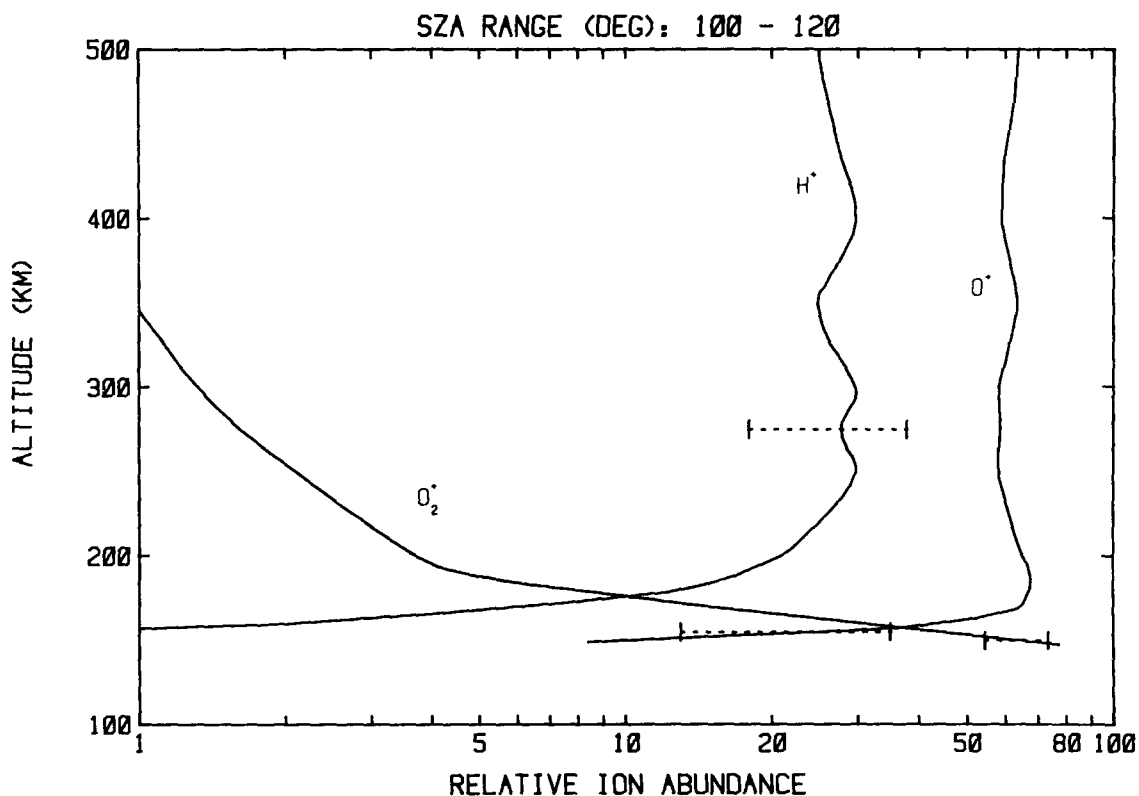


Figure 7-19. VIRA Model Ionosphere - Relative Abundances of H^+ , O^+ , and O_2^+ , $100^\circ < \text{SZA} < 120^\circ$

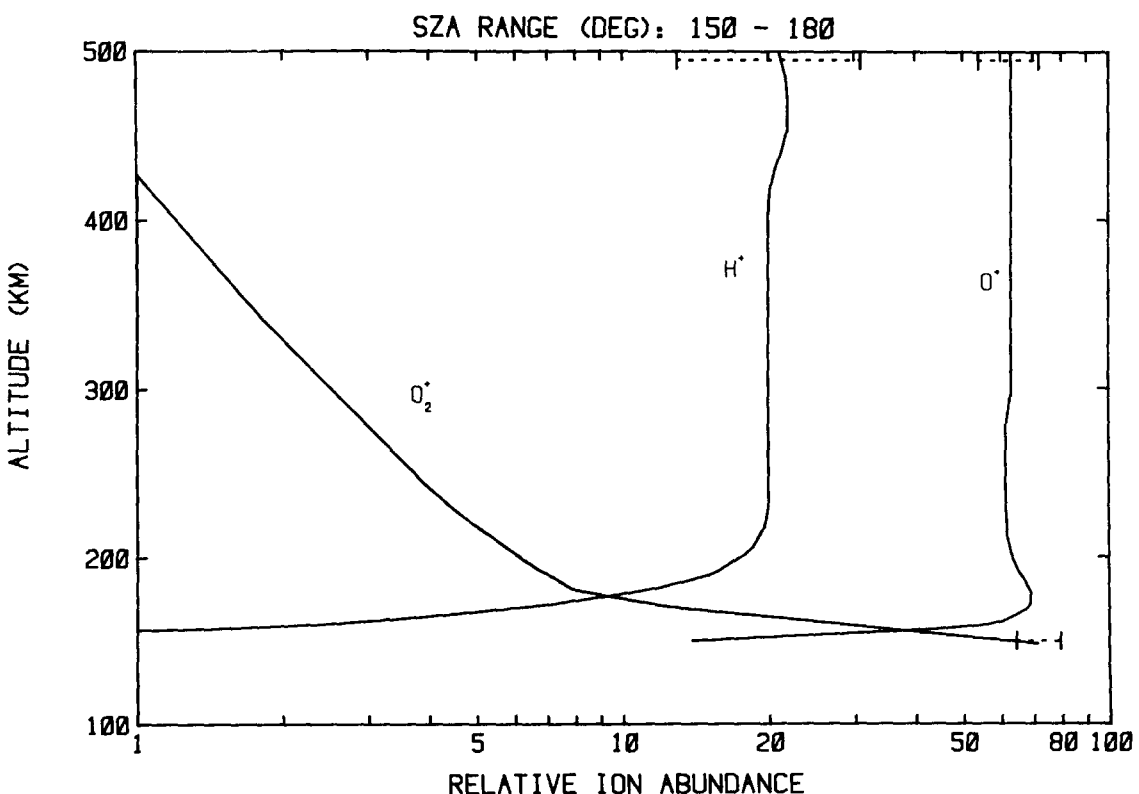


Figure 7-20. VIRA Model Ionosphere - Relative Abundances of H^+ , O^+ , and O_2^+ , $150^\circ < \text{SZA} < 180^\circ$